THE JOURNAL OF BIOLOGICAL CHEMISTRY VOL. 291, NO. 11, pp. 5844–5859, March 11, 2016

The Nutrient and Energy Sensor Sirt1 Regulates the Hypothalamic-Pituitary-Adrenal (HPA) Axis by Altering the Production of the Prohormone Convertase 2 (PC2) Essential in the Maturation of Corticotropin-releasing Hormone (CRH) from Its Prohormone in Male Rats*

Received for publication, July 6, 2015, and in revised form, January 4, 2016 Published, JBC Papers in Press, January 11, 2016, DOI 10.1074/jbc.M115.675264

Anika M. Toorie[‡§], Nicole E. Cyr[‡¶], Jennifer S. Steger[‡], Ross Beckman[‡], George Farah[¶], and Eduardo A. Nillni[‡‖1]

From the [‡]Division of Endocrinology, Department of Medicine, The Warren Alpert Medical School of Brown University/Rhode Island Hospital, Providence, Rhode Island 02903, the [§]Graduate Program in Pathobiology and [‖]Department of Molecular Biology, Cell Biology, and Biochemistry, Brown University, Providence, Rhode Island 02903, and the [¶]Biology Department and Neuroscience Program, Stonehill College, Easton, Massachusetts 02357

Understanding the role of hypothalamic neuropeptides and hormones in energy balance is paramount in the search for approaches to mitigate the obese state. Increased hypothalamic-pituitary-adrenal axis activity leads to increased levels of glucocorticoids (GC) that are known to regulate body weight. The axis initiates the production and release of corticotropin-releasing hormone (CRH) from the paraventricular nucleus (PVN) of the hypothalamus. Levels of active CRH peptide are dependent on the processing of its precursor pro-CRH by the action of two members of the family of prohormone convertases 1 and 2 (PC1 and PC2). Here, we propose that the nutrient sensor sirtuin 1 (Sirt1) regulates the production of CRH post-translationally by affecting PC2. Data suggest that Sirt1 may alter the *preproPC2* gene directly or via deacetylation of the transcription factor Forkhead box protein O1 (FoxO1). Data also suggest that Sirt1 may alter PC2 via a post-translational mechanism. Our results show that Sirt1 levels in the PVN increase in rats fed a high fat diet for 12 weeks. Furthermore, elevated Sirt1 increased PC2 levels, which in turn increased the production of active CRH and GC. Collectively, this study provides the first evidence supporting the hypothesis that PVN Sirt1 activates the hypothalamic-pituitary-adrenal axis and basal GC levels by enhancing the production of CRH through an increase in the biosynthesis of PC2, which is essential in the maturation of CRH from its prohormone, pro-CRH.

Since its discovery in 1981 (1), corticotropin-releasing hormone (CRH)[2] has been demonstrated to be involved in mediating various physiological processes, including those involved in organismal homeostasis. Renowned for its critical role in mediating the stress response (2), CRH functions to regulate metabolic, immunologic, and homeostatic changes both basally and under various pathologic conditions (3–5). CRH heterogeneously expresses in the periphery and the brain with high expression in the hypothalamic paraventricular nucleus (PVN) (6–8). Arginine vasopressin (AVP) is also produced in the PVN and acts to synergize CRH actions. It is the CRH that is produced in the medial parvocellular division of the PVN that functions as the central regulator of the HPA axis (9).

Levels of bioactive CRH are dependent on the post-translational processing of its precursor pro-CRH. Prohormone post-translational processing is the mechanism by which all peptide hormones become biologically active (10, 11). In rodents and humans, aberrations in prohormone processing results in deleterious health consequences, including metabolic dysfunctions (12–17). CRH is initially produced as a large inactive precursor, *preproCRH*, that is made of 196 amino acids (18, 19). After cleavage of the signal sequence, the prohormone (pro-CRH) enters the lumen of the rough endoplasmic reticulum and is routed to the trans-Golgi network where it undergoes enzymatic post-translational modifications to generate several intermediate forms as well as the bioactive CRH(1–41) peptide that is produced from the C-terminal region of the precursor polypeptide (20). Specifically, pro-CRH is cleaved by prohormone convertase 2 (PC2) or PC1 at Arg-152–Arg-153, thereby releasing a 43-residue CRH peptide (20–22). The PC2 protease is synthesized as a zymogen that undergoes its own post-translational processing autocatalytic maturation within the secretory pathway. CRH is further processed into its bioactive form via the removal of the C-terminal lysine residue by the actions of carboxypeptidase E (CPE), and it is subsequently amidated at the exposed carboxyl group of a glycine residue by peptidylglycine hydroxylase (also referred to as peptidylglycine α-amidating monooxygenase) (Fig. 1) (23).

* This work was supported by National Institutes of Health GrantwR01 DK085916 and DK085916S from NIDDK (to E.A.N.) and the Dr. George A. Bray Research Scholars Award (to N. E. C.). The authors declare that they have no conflicts of interest with the contents of this article. The content is solely the responsibility of the authors and does not necessarily represent the official views of the National Institutes of Health.

[1] To whom correspondence should be addressed: Brown University. 40 Pine Grove Ave, Sharon, MA 02067. Tel.: 781-784-8525 or 617-755-3621; E-mail: Eduardo_Nillni@Brown.edu.

[2] The abbreviations used are: CRH, corticotropin-releasing hormone; PVN, paraventricular nucleus; GC, glucocorticoid; HPA, hypothalamic-pituitary-adrenal; PC, prohormone convertase; qrtPCR, quantitative real time PCR; RIA, radioimmunoassay; DIO, diet-induced obese; T_3, triiodothyronine; T_4, thyroxine; AVP, arginine vasopressin; CPE, carboxypeptidase E; GC, glucocorticoid; HFD, high fat diet; ME, median eminence; POMC, pro-opiomelanocortin; ARC, arcuate nucleus of the hypothalamus; α-MSH, α-melanocyte-stimulating hormone; TRH, thyrotropin; releasing hormone.

Under both basal and stimulated conditions, CRH produced in the PVN is released from nerve terminals that anteriorly juxtapose the median eminence where it is traversed into the hypothalamo-hypophyseal portal system (24). Upon binding to its cognate receptor, corticotropin-releasing hormone receptor 1 (CRHR1) (25), which is expressed by corticotropic cells of the adenohypophysis, CRH stimulates the synthesis and secretion of adrenocorticotropic hormone (ACTH) as well as other bioactive molecules such as β-endorphin (26). ACTH engages the melanocortin 2 receptor expressed by cells of the adrenal cortex and stimulates the production and secretion of steroid hormones such as GC (27).

Both ACTH and glucocorticoids (GCs) function to regulate the HPA axis activity via long and short negative feedback loops that signal at the level of the hypothalamus, extra-hypothalamic brain sites, and the adenohypophysis. CRH functions to promote negative energy balance by suppressing appetite and enhancing thermogenesis (28–30), and the GC functions to promote positive energy balance in part by affecting glucose metabolism, lipid homeostasis, and increasing appetite drive (31). Although a consensus on the exact role of adrenal activity in relation to energy dysfunction has yet to be reached, increased and sustained basal GC is implicated in the development of visceral obesity, insulin resistance, and metabolic disease (32–34).

Silent mating type information regulation 2 homolog 1 (Sirt1) is a NAD^+-dependent class III deacetylase that regulates gene expression and protein activity via the deacetylation of its effector targets, which include histones and transcription factors. Sirt1's dependence on NAD^+ supports its role as an energy sensor (35), and several studies have demonstrated that Sirt1 is nutrient-sensitive and plays a role in energy balance both in the periphery and in the brain (36–39). Studies from our laboratory and others had demonstrated that reducing central Sirt1 level or activity resulted in decreased food intake and body weight gain in lean rodents (36, 37, 40), whereas pharmacological activation of ARC Sirt1 resulted in increased food intake and body weight gain (36).

Moreover, inhibition of central Sirt1 activity conferred an anorectic response specifically via enhanced melanocortin signaling and melanocortinergic tone, respectively, (36, 37). In addition, we demonstrated that Sirt1 protein is increased in the ARC of diet-induced-obesity (DIO) rodents. In that same study, central inhibition of Sirt1 activity enhanced melanocortin signaling, increased thyroid activity and energy expenditure, and was associated with reduced overnight body weight gain independent of alterations in food consumption (40). In another study, pan-neuronal knock-out (limited to neurons of the central nervous system) of functional Sirt1 resulted in enhanced peripheral and central insulin sensitivity (41). Collectively, these findings suggest that reducing hypothalamic Sirt1 activity can promote negative energy balance and protect against the development of type 2 diabetes and obesity.

In this study, we investigated the role of PVN Sirt1 on CRH production from its precursor under different nutritional conditions and the resulting impact on energy balance. We utilized a combination of *in vitro* experiments as well as an *in vivo* model wherein we pharmacologically manipulated central and PVN Sirt1 activity in lean rats and the Sprague-Dawley model of adult-onset DIO.

Experimental Procedures

Animals and Diets—Male Sprague-Dawley rats (22 days old) were purchased from Harlan Laboratories (Wilmington, MA) and fed a standard chow (Purina Lab Chow number 5001) or a high-fat diet (HFD) (Rodent Chow number D12492, Research Diets) for 12 weeks. The regular diet provided 3.3 kcal/g energy (59.8% carbohydrate, 28.0% protein, and 12.1% fat). The HFD provided 5.24 kcal/g energy (20.0% carbohydrate, 20.0% protein, and 60.0% fat). DIO rats were considered those individuals maintained on HFD for 12 weeks whose body weight was greater than the mean plus 3 standard deviations of the lean group fed standard chow. DIO-resistant rats were excluded from our studies and are considered those rats that were maintained on a high fat diet for 12 weeks whose body weight was not greater than the mean plus 3 standard deviations of the lean group fed standard chow (42). We previously described the hormonal and physiological characteristics of the rat DIO model (43). Rats were fasted for 24 h in experiments investigating Sirt1 protein content in the PVN. Animals were fasted because Sirt1 is known to increase with fasting and therefore can be measured easily via Western blot. Importantly, in all other experiments animals had *ad libitum* access to food to mitigate the stress response incurred by fasting, thus excluding confounding stress-induced GC levels. This procedure has been used in previous studies (40). The Institutional Animal Care and Use Committee of Rhode Island Hospital/Brown University approved all experimental protocols and euthanasia procedures.

Surgeries and Drugs—Animals were weighed and anesthetized with intraperitoneal (i.p.) injections of 50 mg/kg ketamine and 0.25 mg/kg dormitor and prepared for stereotaxic implantation of an intra-cerebroventricular (icv) 21-gauge stainless steel guide cannula (Plastic One, Roanoke, VA), according to coordinates obtained from Paxinos and Watson atlas into the lateral ventricle: anteroposterior, −0.8 mm; lateral, −1.2 mm; and ventral, −3.6 mm. Guide cannulae were assessed for correct placement by monitoring water intake upon administration of angiotensin II (40 ng/rat; Sigma). For intra-PVN studies, rats were stereotaxically implanted with a 22-gauge stainless steel double guide cannula (Plastic One) using the following coordinates: anteroposterior, −1.9 mm; lateral, ±0.5 mm; and ventral, −7.3 mm (44); internal cannula extended 0.5 mm beyond the cannula guide, and placement was verified by india ink infusion. All infusions were performed on free-moving animals using a 30-gauge needle where the injection tip was connected by polyethylene tubing to a 25-μl Hamilton syringe. Animals were given, minimally, 7 days to recover from surgery for all experiments. Additionally, animals were handled and cannulae were inserted daily for 10 days post-surgery to acclimate animals and mitigate the stress response on the day of the experiment.

Ex-527 (Sigma) was used for Sirt1 inhibition experiments because it has been shown to very specifically inhibit Sirt1 enzymatic activity and to elicit changes in POMC and body weight when given icv in rats (36, 40). For these experiments, lean and DIO rats were given either an intra-lateral ventricle infusion or

intra-PVN infusion of either vehicle control or Ex-527 (5 μg in vehicle). In another experiment, we infused the Sirt1-activating compound, resveratrol (5 μg in vehicle), into the lateral ventricles of lean fed rats. Because of the promiscuous nature of resveratrol, in subsequent experiments the Sirt1-specific activating compound, SA3 (Sirtuin activator 3/CAY10591; 3–6 μg in vehicle), was infused into the PVN of lean and DIO rats. Resveratrol was infused into the lateral ventricle at 9 a.m. and 4 p.m. on day 1, and animals were sacrificed at 9 a.m. on the subsequent day. For all remaining experiments, infusions were performed between 3 p.m. and 5 p.m. on day 1 and again the following morning beginning at 8 a.m. to 12 p.m. as indicated, and animals were euthanized a few hours later. For Sirt1 inhibition experiments, it was important to fast the rats so that all rats would have high Sirt1 on which the inhibitor could work. In contrast, it was important not to elevate Sirt1 by fasting during Sirt1 activator (SA3) studies so that the rats given SA3 would increase Sirt1 activity in the PVN compared with vehicle controls. This procedure has been used in previous studies (40).

Sample Collection and Preparation—PVN (bregma −1.3 to −2.3 mm) and ARC/median eminence (ME) (bregma −2.5 to −3.5 mm) samples were microdissected and frozen immediately in liquid nitrogen and kept at −80 °C (40). Trunk blood samples were taken to isolate serum to analyze for GC, ACTH, and levels of the thyroid hormones triiodothyronine (T_3) and thyroxine (T_4). The pituitary was also collected and the anterior/intermediate lobes dissected from the posterior lobe. Samples were subjected to the following: peptide extraction with 2 N acetic acid supplemented with a protease inhibitor mixture to measure ACTH by specific RIA; homogenization in 0.15 M PBS supplemented with sodium azide and protease inhibitor mixture to measure CRH by a specific CRH RIA (Phoenix Pharmaceuticals); protein extraction with RIPA buffer (50 mM Tris-HCl, pH 7.4, 150 mM NaCl, 0.5% sodium deoxycholate, 0.1% SDS, 1% Nonidet P-40) supplemented with protease inhibitor mixture for Western blot analysis; and RNA isolation using TRIzol reagent according to the manufacturer's suggestion (Molecular Research Center, Cincinnati, OH) for RT-qrtPCR. For all studies, all analyses (RIA, Western blotting, and RT-qrtPCR) were performed on samples taken from individual rats; samples were not pooled.

Oxygen Consumption and Food Intake—Oxygen consumption was measured using a customized Oxymax system (Columbus Instruments, Columbus, OH). Rats were placed in individual calorimetry chambers 2 h before sampling. Samples were taken every 6 min thereafter, and the first 2 h of sampling data were excluded for the final analysis. For Ex-527 experiments, rats were placed in chambers immediately following the first infusion. Rats were taken out of the chamber the next morning at 1100 h and were again infused. Animals were allowed free access to food and water at all times. Oxygen consumption comparisons were made between lean rats with and without Sirt1 manipulation and between DIO rats with and without Sirt1 manipulation separately. Thus, within each diet group, the surface area and body composition did not differ, which is known to affect energy expenditure (45). However, oxygen consumption data were normalized to body weight for each individual. For food intake measurement, chow was measured prior to infusion and post-sacrifice. Overnight food consumption is presented as the net amount of food intake and was determined by subtracting the post-sacrifice food weight from the initial weight of food.

In Vitro Studies—We began *in vitro* studies in the murine N43-5 hypothalamic POMC-positive cell line (CELLutions Biosystem) to investigate the effect of Sirt1 manipulation on the levels of the prohormone convertases. We subsequently transitioned to the murine corticotroph tumoral AtT20 cell line (ATTC) for the remainder of our *in vitro* studies wherein we investigated Sirt1's regulation of CRH production because these cells, when transfected with *preproPC2* cDNA, can produce α-MSH (46, 47), whereas N43-5 cells do not, indicating that the PC2 produced by N43-5 cells are not biologically functional. Both N43-5 and AtT20 cells were cultured in DMEM (Dulbecco's modified Eagle's medium; Invitrogen, Life Technologies, Inc.) supplemented with 10% of fetal bovine serum, 100 units/ml penicillin, and 10 μg/ml streptomycin. To measure intracellular and released CRH content, cells were transiently co-transfected with a *CMV* plasmid containing *preproPC2* cDNA and a *CMV* plasmid containing *preproCRH* cDNA (Origene). For Sirt1-knockdown experiments, we transfected AtT20 cells with control or Sirt1 small hairpin RNA (shRNA), kindly provided by Dr. Pere Puigserver (Dana-Farber Cancer Institute, Department of Cell Biology, Harvard Medical School) and described previously (48). To enhance Sirt1 levels, AtT20s were transfected with *Sirt1* cDNA (Addgene, Cambridge, MA). Both cDNA and shRNA transfections were performed using Lipofectamine 2000 (Invitrogen) following the manufacturer's instructions. Briefly, cells were incubated with the cDNA (4 μg)-Lipofectamine complex for 6 h in serum-free media. The medium was changed to DMEM for overnight incubation. For knockdown studies, we used 1 μg of shRNA and antibiotic/serum-free DMEM. N43-5 cells were collected in HEPES-KOH buffer (20 mM HEPES, 125 mM NaCl, 1 mM EDTA, 20 mM NaF, 0.1% Triton X, 0.1% Nonidet P-40). AtT20 cells were lysed and collected in RIPA buffer supplemented with protease inhibitor mixture for Western blot analysis or 0.15 M PBS with 0.5% NaN_3 supplemented with protease inhibitor mixture for CRH analysis, and media were collected and supplemented with protease inhibitor mixture to measure CRH by RIA.

RIA and Glucose Assay—RIA analysis of ACTH, T_3, and T_4 were performed as described previously (46). CRH was measured using a commercial CRF RIA kit from Phoenix Pharmaceuticals (Burlingame, CA). Plasma thyroid hormones were measured using commercial RIA kits from MP Biomedicals Diagnostic Division (Orangeburg, NY) as described previously (36). The sensitivity of the T_3 and T_4 assays were 25 ng/dl and 1.2 mg/dl, and the intra- and inter-assay variabilities were ~5–7% and 10–11%, respectively. The ACTH RIA was performed using our in-house anti-ACTH antiserum (1:30,000) and 5000 cpm of ^{125}I-ACTH tracer. The sensitivity of the assays was ~10.0 pg/tube, and the intra- and inter-assay variabilities were ~5–7 and 10–11%, respectively. Plasma GC was measured using a commercial rat and mouse GC RIA kit from MP Biomedicals Diagnostic Division (Orangeburg, NY). The sensitivity was 7.7 ng/ml, and the intra- and inter-assay variabilities were 4–10 and 6.5–7%, respectively. Insulin was measured

using a rat insulin RIA kit from Millipore (catalog no. RI-13K), and glucose was measured utilizing a Quanti Chrom glucose assay kit from Bioassay Systems (catalog no. DIGL-100) according to the manufacturer's suggestions.

Western Immunoblotting—Protein samples (30 μg) were separated on an 8 or 12% acrylamide gel and transferred onto a PVDF membrane. Precision Plus Protein standards were used as molecular weight markers (Bio-Rad). Membranes were washed in PBS with 0.1% Tween 20 (PBS-T) and then blocked with 5% BSA for 60 min. Membranes were then probed with a primary antibody overnight at 4 °C. PC1 and PC2 protein was detected by Western blot via the use of specific primary antibodies (1:10,000 dilution, each), which had been characterized in a previous study (49). We used anti-ACTH and anti-α-MSH antibodies custom-made in our laboratory to identify the POMC precursor (31 kDa) (15). Other antibodies used were as follows: FoxO1 (1:500), Sirt1 (1:1000), and CPE (1:500) from Cell Signaling Technology (Danvers, MA); acFoxO1 (1:200) and β-actin (1:10,000) as a loading control from Santa Cruz Biotechnology (Dallas, TX). Membranes were washed in PBS-T (three times for 5 min) and incubated in the appropriate secondary antibody for 60 min the following day. Membranes were then incubated with enhanced chemiluminescence buffer for 1 min and visualized using the Alpha Innotech imaging system (ProteinSimple). Band density was analyzed using the ImageJ software program (National Institutes of Health).

Quantitative Real Time PCR—Total RNA was extracted from ARC and PVN samples. cDNA was prepared from 1 μg of total RNA using random hexamer primers and SuperScript III reverse transcriptase (Invitrogen). RT-qrtPCRs included 100 ng of cDNA as template, 200 nM of our target gene or tubulin primers, and Power SYBR Green PCR Master Mix (Applied Biosystems-Life Technologies). An ABI Prism 7500 FAST sequence detector (Applied Biosystems) was used to amplify reactions and generate standard curves. Values were normalized to tubulin. The $\Delta\Delta CT$ method was used for relative quantification and statistical analysis. Primer sequences used for RT-qrtPCR are available upon request.

Statistical Analysis—The results for each treatment are presented as mean ± S.E. A two-tailed *t* test was used to analyze differences between two groups. An analysis of variance, followed by Tukey's HSD post hoc test, was used to analyze differences between more than two groups. A Shapiro-Wilk W goodness-of-fit test was used to test for normal distributions, and Levene's test (two-group comparisons) or Bartlett's test (comparisons between more than two groups) was used to test for homogeneous variances in all variables. For variables with non-normal distributions and unequal variances, a nonparametric Mann Whitney *U* test or Kruskal-Wallis test was used. Differences were considered to be significant at $p < 0.05$. Prizm (version 4.0b GraphPad Software, Inc., La Jolla, CA). Statistics for each comparison are presented in the figure legends.

Results

DIO Rodents Display Increased PVN Sirt1 and Basal GC; Central Sirt1 Manipulation Alters PVN PC2 Levels and Basal GC—Similar to DIO ARC Sirt1 content (40), Sirt1 protein is also elevated in the PVN of DIO rats compared with their lean controls (Fig. 1*A*). In addition, lean and DIO rats retained a circadian expression profile of basal GC with low levels observed in the morning, which is the inactive period for nocturnal animals, and higher levels observed later in the day (50). However, as compared with their lean counterparts, DIO rats displayed elevated serum GC both in the morning (Fig. 1*B*) and in the afternoon (Fig. 1*C*). We then investigated the effects of increasing central Sirt1 activity on basal GC concentrations in lean rats. In lean rats, resveratrol was infused centrally to increase Sirt1 activity and resulted in a significant increase in basal GC levels (Fig. 1*D*), yet did not alter CRH mRNA (Fig. 1*E*), suggesting that the Sirt1-inducted increase in GC was not due to changes in CRH transcription.

Consequently, we explored whether Sirt1's effect on GC was mediated via changes in the processing enzymes responsible for the cleavage of pro-CRH into its bioactive form (Fig. 1*F*). Accordingly, lean and DIO rats were treated to centrally inhibit Sirt1 activity, and PC1 and PC2 protein was assessed from PVN samples. PC2 protein was significantly reduced in the PVN of DIO rodents with central Sirt1 inhibition (Fig. 1*G*) relative to their vehicle-infused control, an effect that was not observed in lean rats (Fig. 1*J*). In contrast, central Sirt1 inhibition resulted in no significant changes in PC1 protein in the PVN of either DIO (Fig. 1*H*) or lean rodents (Fig. 1*K*). There were no differences in CRH expression within the PVN of DIO (Fig. 1*I*) or lean (Fig. 1*L*) rats with or without central Sirt1 inhibition. Collectively, these results suggest that DIO individuals develop a Sirt1-mediated increase in basal GC and that these effects are likely mediated via its regulation of PC2, which enhances the post-translational processing of pro-CRH.

Sirt1 Manipulation Positively Affects CRH Production in Vitro—We used an *in vitro* system to validate the above results and further characterize Sirt1's regulation of CRH. We first assessed whether Sirt1 affected the levels of the PCs. Sirt1 overexpression (Fig. 2*A*) significantly increased pro-PC2 (Fig. 2*B*) as well as pro-PC1 (Fig. 2*C*) protein in N43-5 cells. Consistent with this observation, an shRNA-mediated decrease in Sirt1 protein (Fig. 2*D*) decreased both PC2 (Fig. 2*E*) and PC1 (Fig. 2*F*) levels in AtT20 cells. Of note, and as reported previously (40), we observed diminished CPE protein and increased CPE protein levels in AtT20 cells with Sirt1 overexpression and knockdown, respectively (data not shown).

To validate the specificity of Sirt1's regulation of the PCs, we overexpressed AtT20 cells with *Sirt1* and *preproPC2* cDNAs and treated them with Ex-527 to inhibit Sirt1 activity or with vehicle control. AtT20 cells transfected with Sirt1 (Fig. 3*A*) displayed increased PC2 (Fig. 3*B*) and PC1 (Fig. 3*C*) protein. As expected, Sirt1 overexpression increased Sirt1 protein (Fig. 3*A*). However, even with Sirt1 overexpression, Ex-527 significantly reduced Sirt1 protein as well as PC2 protein (Fig. 3*B*) but not PC1 protein (Fig. 3*C*). We then investigated whether Sirt1 manipulation affected CRH production and release. As N43-5 cells do not produce functional PC2, we utilized the AtT20 cell line in which pro-CRH processing had been previously characterized (20, 22, 51). AtT20 cells transfected with cDNAs encoding for *preproCRH* and *preproPC2* were also transfected with Sirt1 or control cDNAs. The results show that Sirt1 overexpression increased PC2 and PC1 protein (Fig. 3,

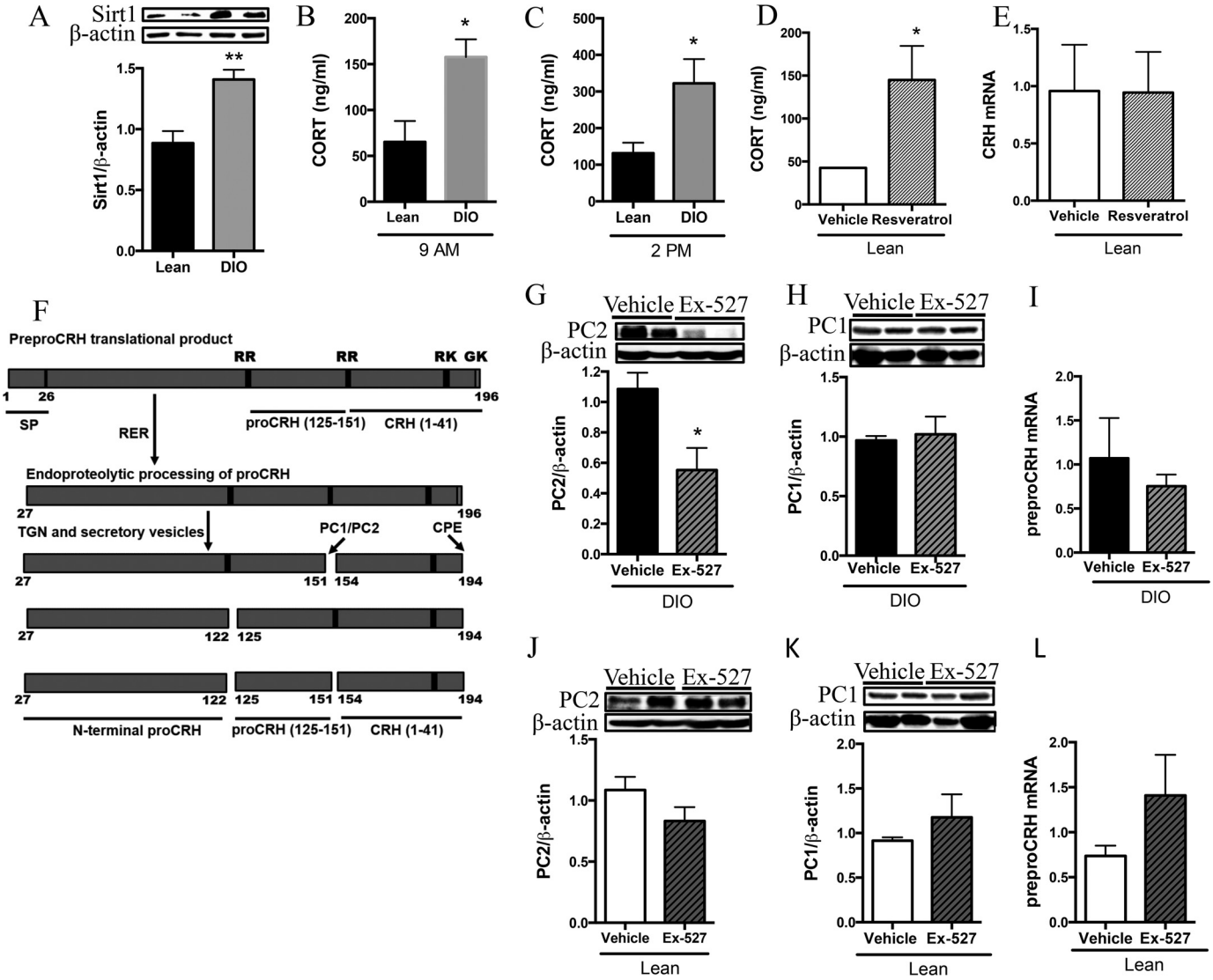

FIGURE 1. **DIO rodents display increased PVN Sirt1 and basal GC.** Rats were fed a diet high in fat for 12 weeks to generate DIO (*gray bars*) rodents, whereas lean controls were maintained on standard chow (*black bars*). *A,* lean and DIO rats were fasted for 24 h and sacrificed, and the PVN was collected and subjected to Western blot analysis for Sirt1 protein levels ($n = 6$/group). **, $p < 0.01$. *B* and *C,* lean and DIO rats were sacrificed either in the morning or mid-afternoon and trunk blood was collected and serum-extracted, and GC (ng/ml) was measured by RIA. *B,* 9 a.m. basal GC ($n = 4$ lean and 5 DIO). *C,* 2 p.m. basal GC ($n = 7$ lean and 10 DIO). *D* and *E,* lean rats were icv-infused twice with 5 μg of resveratrol or vehicle control at 9 a.m. and 4 p.m. on day 1. Rats were sacrificed at 9 a.m. the following day; serum was isolated from trunk blood and measured for GC. *D,* serum GC levels ($n = 3$/group). *E,* PVN was assessed for CRH mRNA ($n = 4$/group). *F,* pro-CRH processing cascade is modeled here and has been described previously. *G–J,* lean and DIO rats were icv-infused with 5 μg of Ex-527 or vehicle control at the beginning of the fasting period and again 8 h later. Rats were fasted for 24 h total and sacrificed, and the PVN was collected and processed for protein or mRNA analysis. *G–L,* PC2 protein and PC1 protein ($n = 6$/group) and *CRH* mRNA from the PVN of lean and DIO rats with or without central Sirt1 inhibition. *G,* PC2 in DIO PVN. *H,* PC1 in DIO PVN. *I,* CRH mRNA in DIO PVN ($n = 3$ vehicle and 4 Ex-527). *J,* PC2 in lean PVN. *K,* PC1 in lean PVN. *L,* CRH mRNA in lean PVN. ($n = 4$/group). Data are mean ± S.E. *, p value < 0.05.

D–F), which was associated with enhanced intracellular CRH content (Fig. 3*G*), as well as an increase in CRH released into the media (Fig. 3*H*).

In other experiments, AtT20 cells transfected with *prepro-CRH* and *preproPC2* cDNA and treated with resveratrol (a stimulator of Sirt1) displayed an increase in PC2 (Fig. 4*A*) and PC1 (Fig. 4*B*). This observation was associated with an intracellular increase in CRH (Fig. 4*C*) and an increase in CRH released into the media (Fig. 4*D*). We also treated AtT20 cells with SA3, a Sirt1-specific activator, to confirm the specificity of the above results. Cells treated with SA3 to specifically enhance Sirt1 activity displayed increased PC2 and PC1 protein levels (Fig. 4, *E* and *F*), and this was again associated with increased intracellular and released CRH content (Fig. 4, *G* and *H*). Furthermore, Sirt1-specific inhibition resulted in decreased PC2 (Fig. 4*I*) and PC1 (Fig. 4*J*) and was associated with reduced intracellular CRH content (Fig. 4*K*); however, we did not detect changes in the amount of CRH released into the media (Fig. 4*L*). Together, these results suggest that Sirt1 overexpression or activation induces CRH production and release, an effect that is mediated through Sirt1 actions on PC1 and PC2.

Sirt1 Activation in the PVN Positively Affects Adrenal Activity in Vivo—We then investigated the positive stimulation of PVN Sirt1 in lean and DIO rodents. Because resveratrol is known to have off-target effects, rats were intra-PVN infused with SA3, to specifically enhance Sirt1 activity. Increasing the activity of

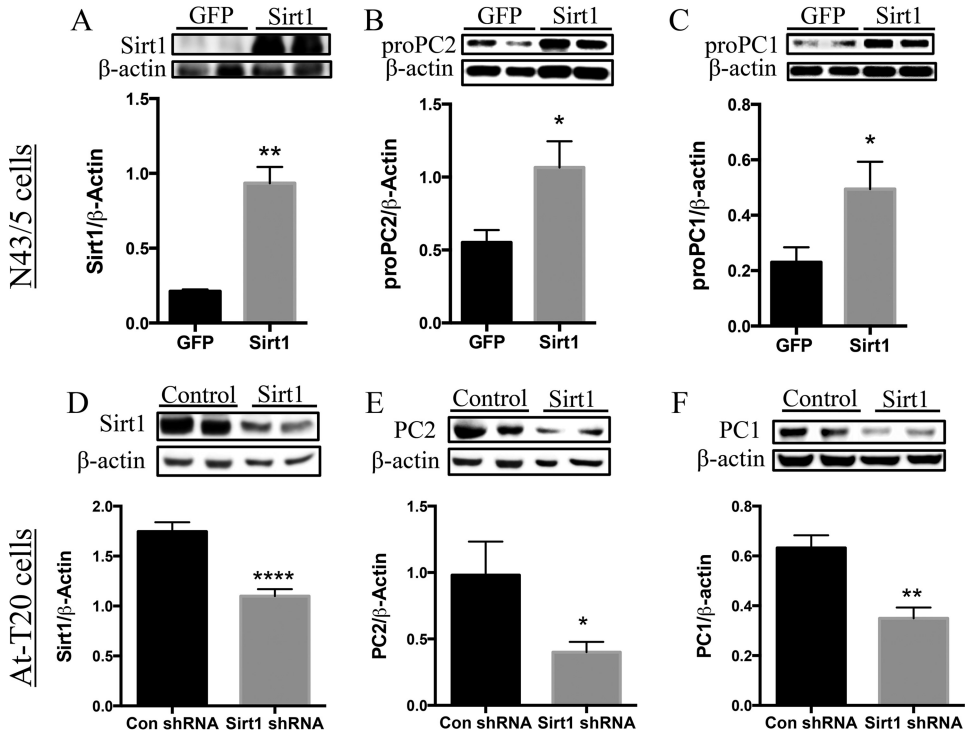

FIGURE 2. **Sirt1 regulates PC1 and PC2 expression in N43-5 and AtT20 cells.** *A–C,* N43-5 cells were transfected with 4 μg of Sirt1 cDNA to increase the expression of Sirt1, and cells were collected 48 h post-transfection. *A,* Sirt1 protein ($n = 6$/group). *B,* pro-PC2 ($n = 6$/group). *C,* pro-PC1 ($n = 6$/group). These results were repeated in an independent experiment with the same response. *D–F,* AtT20 cells were transfected with an shRNA targeted against Sirt1 or control shRNA and collected 72 h post-transfection. *D,* Sirt1 protein ($n = 6$ control shRNA and 11 Sirt1 shRNA). *E,* PC2 protein ($n = 5$ control shRNA and 7 Sirt1 shRNA). *F,* PC1 protein ($n = 5$ control shRNA and 7 Sirt1 shRNA). Data are mean ± S.E. *, p value < 0.05; **, p value < 0.01; ****, p value < 0.00001.

Sirt1 in the PVN of lean rodents resulted in elevated serum GC (Fig. 5*A*) and ACTH (Fig. 5*B*) levels but did not alter serum T_3 (Fig. 5*C*) or T_4 (Fig. 5*D*) levels in comparison with vehicle-infused controls. We assessed the anterior pituitaries of these rodents for changes in POMC, from which ACTH is derived, and CPE and PC1, the primary enzymes that catalyze the cleavage of POMC into ACTH, as these are indicators of CRHR1 stimulation. Stimulating PVN Sirt1 activity in lean rodents increased pituitary POMC (Fig. 5*F*), PC1 (Fig. 5*G*), and CPE (Fig. 5*H*) but did not change ACTH content (Fig. 5*E*), most likely because ACTH was released to serum (Fig. 6*B*).

Similarly, DIO rodents with PVN Sirt1 activation displayed elevated serum GC (Fig. 6*A*) and ACTH (Fig. 6*B*), with no alterations in T_3 (Fig. 6*C*) or T_4 (Fig. 6*D*) levels compared with vehicle controls. In addition, POMC (Fig. 6*F*), PC1 (Fig. 6*G*), and CPE (Fig. 6*H*) proteins were increased in the anterior pituitary of these individuals; however, we saw no alterations in the amount of ACTH within their anterior pituitary (Fig. 6*E*) when compared with their respective controls. Collectively, these results indicate that Sirt1 activation in the PVN functions to regulate, in a positive manner, hypophysiotropic adrenal activity but not hypophysiotropic thyroid activity.

Sirt1 Inhibition in the PVN Reduces Adrenal Activity in DIO—We then assessed the effect of acute PVN Sirt1 inhibition on hypophysiotropic adrenal activity in lean and DIO rats and its subsequent effect on food intake and energy expenditure. Inhibition of Sirt1 in the lean state did not alter PVN PC2 (Fig. 7*A*), PC1 (Fig. 7*B*), or CPE (Fig. 7*C*) proteins nor were there changes in the quantity of CRH in either the PVN (Fig. 7*D*) or the ME (Fig. 7*E*). There were also no changes in GC (Fig. 7*F*), T_3 (Fig. 7*G*), T_4 (Fig. 7*H*), glucose (Fig. 7*I*), or insulin (Fig. 7*J*) levels. In contrast to our prior observation in regard to food intake in lean rats with central Sirt1 inhibition (36, 40), lean rats with PVN Sirt1 inhibition did not display alterations in overnight food consumption (Fig. 7*K*), energy expenditure (Fig. 7*L*), or body weight change (Fig. 7*M*) relative to their vehicle controls.

In contrast to observations in lean animals, DIO rodents intra-PVN-infused with Ex-527 displayed reduced PVN PC2 (Fig. 8*A*) in comparison with the vehicle control; however, there were no differences in PC1 (Fig. 8*B*) or CPE (Fig. 8*C*) protein. In addition, CRH levels were unchanged between the PVN of DIO rodents with or without PVN Sirt1 inhibition (Fig. 8*D*). However, PVN Sirt1 inhibition in the DIO condition significantly decreased the quantity of CRH localized within the ME (Fig. 8*E*) and significantly reduced serum GC (Fig. 8*F*). Circulating T3 (Fig. 8*G*), T_4 (Fig. 8*H*), and glucose (Fig. 8*I*) levels remained unchanged; yet, insulin concentrations were significantly elevated (Fig. 8*J*) in DIO rodents with PVN Sirt1 inhibition compared with vehicle controls. Different from our prior observations that hypothalamic Sirt1 inhibition throughout the melanocortin system promotes a negative energy balance in DIO by affecting energy expenditure (40), specific inhibition of PVN Sirt1 did not alter food intake (Fig. 8*K*) nor energy expenditure (Fig. 8*L*). However, bodyweight (Fig. 8*M*) was significantly reduced in DIO rodents with Sirt1 inhibition when compared with their vehicle controls. These observations suggest that Sirt1 action in the hypothalamus is tissue-specific.

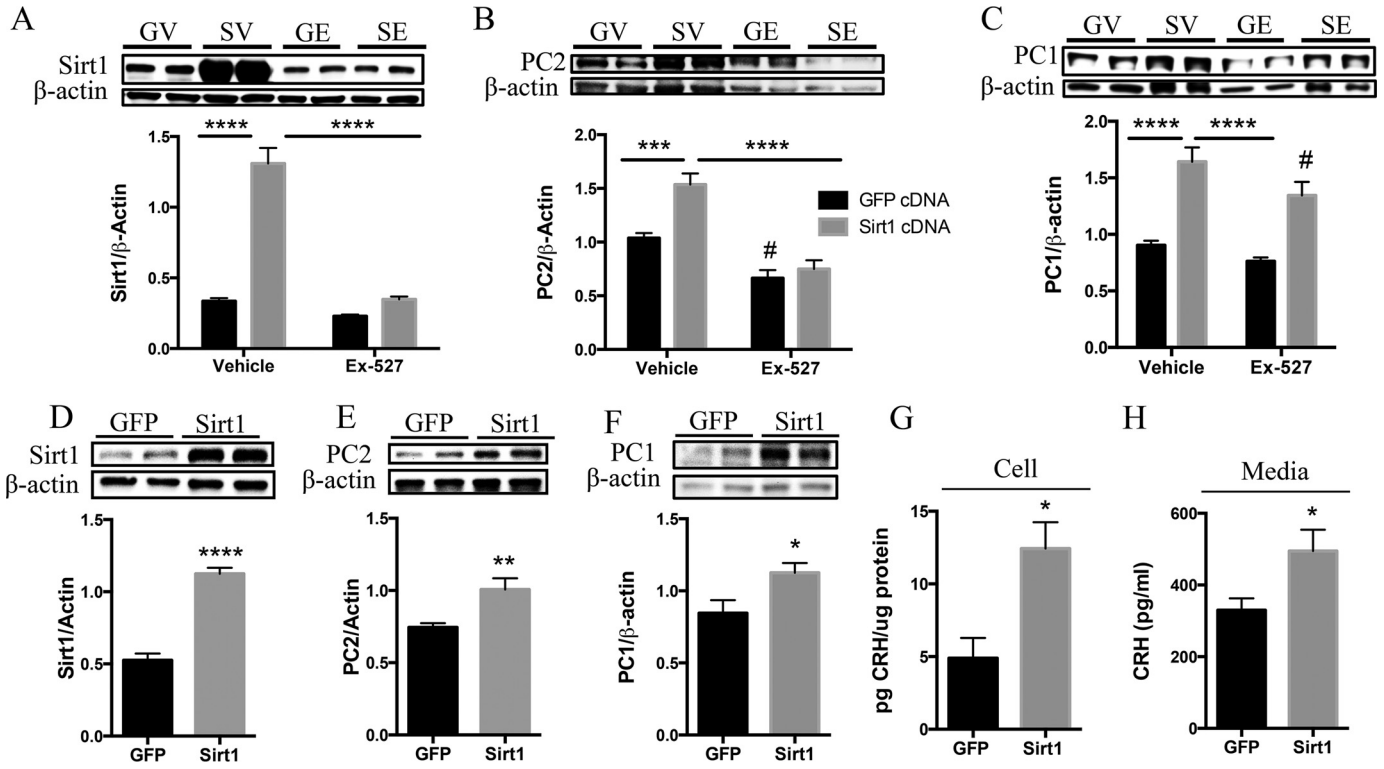

FIGURE 3. **Sirt1 specifically regulates the PCs and CRH production and release in AtT20 cells.** *A–C,* AtT20 cells were co-transfected with 4 μg each of *preproPC2* cDNA and *preproCRH* cDNA alongside either GFP or Sirt1 cDNA and treated 48 h post-transfection with Ex-527 (50 μM) or vehicle control for 6 h. Western blot analysis was performed to measure Sirt1 and PC2 protein levels. *A,* Sirt1 protein (n = 8 GFP-vehicle (*GV*), 8 GFP-Ex527 (*GE*), 10 Sirt1-vehicle (*SV*), and 9 Sirt1-Ex527 (*SE*)). *B,* PC2 protein (n = 11 GFP-vehicle, 13 GFP-Ex527, 10 Sirt1-vehicle, and 10 Sirt1-Ex527). *C,* PC1 (n = 9 GFP-vehicle, 13 GFP-Ex527, 4 Sirt1-vehicle, and 9 Sirt1-Ex527). *D–H,* AtT20 cells were co-transfected with 4 μg of *preproPC2* cDNA and *preproCRH* cDNA alongside either *GFP* or *Sirt1* cDNA and protein lysates assessed for intracellular Sirt1 and PC2 protein and intracellular and released CRH content by Western blot (n = 6/group) and RIA, respectively. *D,* Sirt1 protein. *E,* PC2 protein. *F,* PC1 protein. These results were repeated in two independent experiments with the same response (n = 6/group). *G,* CRH content measured from protein lysates (n = 4 control and 6 Sirt1). *H,* released CRH content (n = 4 control and 6 Sirt1). Data are mean ± S.E. *, p value < 0.05; **, p value < 0.01; ***, p value < 0.001; ****, p value < 0.00001; #, p value < 0.05.

Because pro-PC2 within neuroendocrine cells is synthesized as zymogens that undergo autocatalytic maturation within the secretory pathway, we analyzed whether central Sirt1 inhibition affected its maturation. Inhibition of Sirt1 reduced levels of both pro-PC2 and PC2 with this effect being more pronounced in the latter (Fig. 8*N*). These results suggest that Sirt1 may also regulate the HPA axis by enhancing the processing of pro-PC2 to PC2.

FoxO1 and/or Sirt1 Regulate PC2 in a Positive Manner—Our prior studies revealed that ARC Sirt1 exerted its effect on energy balance partly by modulating the transcription factor FoxO1 (36). Moreover, FoxO1 augments neuropeptide function via its regulation of enzymes involved in the post-translational processing of precursor polypeptides, such as the carboxypeptidase E (CPE) (52). Similarly, both PC1 and PC2 promoter regions contain putative FoxO1-binding elements with consensus sequences for the insulin-response element 5′-TT(G/A)TTTTG-3′ and the related Daf-16 family-binding element (DBE) with 5′-TT(G/A)TTTAC-3′. We also have preliminary data suggesting that the immortalized murine hypothalamic cell line, N43-5, transfected with either PC1-luciferase or PC2-luciferase constructs and treated to inhibit Sirt1 activity resulted in reduced promoter activity for both PC1 and PC2 (data not shown).

Having evidence supporting the role of Sirt1 on FoxO1, and FoxO1 on the PCs, we asked whether Sirt1 increases the biosynthesis of pro-PC2 protein by acting on the *preproPC2* gene or by acting on FoxO1, which in turn acts on the *preproPC2* gene. To this purpose, we measured whether FoxO1 overexpression was sufficient to induce changes in pro-PC1 and/or pro-PC2 levels in the N43-5 cell line, which carries the original promoters of PC1 and PC2. Our results indicate that FoxO1 overexpression (Fig. 9, *A* and *B*) caused an increase in pro-PC2 protein biosynthesis suggesting a positive regulation in the *preproPC2* gene probably by the action of FoxO1 on the *PC2* promoter site. However, pro-PC1 levels remained unchanged (Fig. 9*C*). It is important to point out that, as reported previously (53), FoxO1 mediates an auto feedback loop regulating SIRT1 expression, which was confirmed in our experiment depicted in Fig. 9*D*. These later results pose the question of whether Sirt1 acts upstream of FoxO1 to augment pro-PC2 biosynthesis or whether the positive feedback mechanism described above indirectly results in increased pro-PC2 production via an alternative not yet determined mechanism (*e.g.* post-translational mechanism). It is also possible that Sirt1 regulates PC2 via its actions on another unidentified transcription factor.

To address this question, we next utilized a system where the natural *PC2* promoter is absent. Hence, we transfected the corticotropic AtT0 cells that lacks endogenous *preproPC2*, with *preproPC2* cDNA using a *CMV* promoter. Then, we measured the production of mature PC2 protein. We focused on these sets of experiments only on FoxO1's regulation of PC2, as we

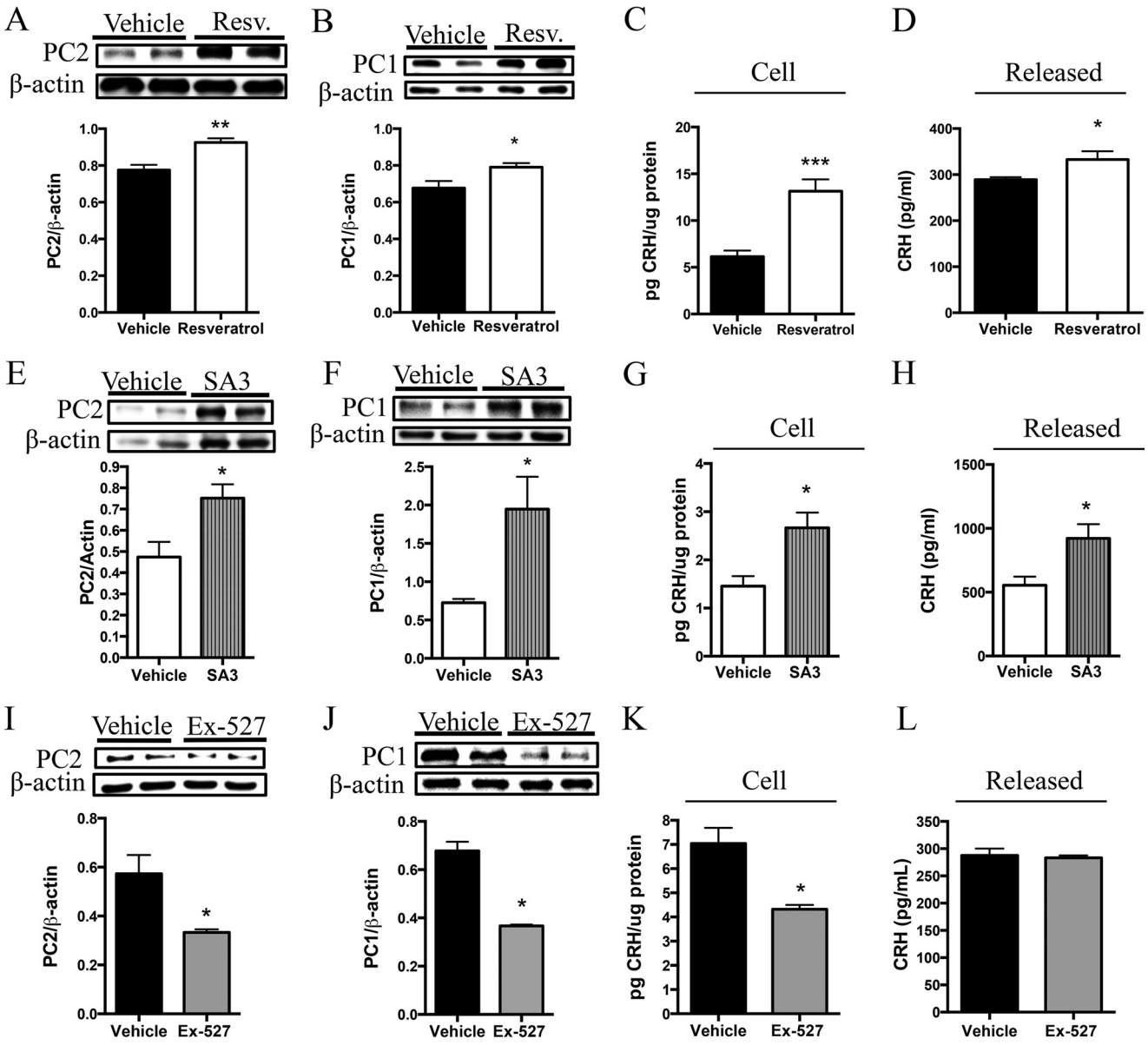

FIGURE 4. **Pharmacological manipulation of Sirt1 activity positively regulates PC1 and PC2 levels alongside correlative changes in CRH production and release.** *A–D,* AtT20 cells were transfected with 4 μg of *preproPC2* cDNA and *preproCRH* cDNA and treated 48 h post-transfection with resveratrol (*Resv.*) (50 μM) for 6 h or with vehicle control, and cells were collected and processed for protein and RIA analysis. Western blot analysis was performed to measure PC2 (n = 6/group) (*A*) and PC1 protein levels (n = 6/group) (*B*). These results were repeated in two independent experiments with the same response, n = 6/condition. *C* and *D,* CRH was measured by RIA to evaluate both cell (n = 6/group) and released (n = 6/group) CRH quantity. *E–H,* in another experiment, AtT20 cells were transfected as described above and treated 48 h post-transfection with SA3 (20 μM) for 6 h or with vehicle control. *E* and *F,* Western blot analysis was performed to measure PC2 (n = 4 vehicle and 6 SA3) and PC1 (n = 4 vehicle and 6 SA3) protein levels. *G* and *H,* CRH measured by RIA to evaluate both released (n = 4 vehicle and 6 SA3) and cellular (n = 4 vehicle and 6 SA3) CRH quantity. *I–K,* AtT20 cells were transfected as aforementioned and treated with Ex-527 (50 μM) or vehicle control for 6 h. *I–L,* Western blot analysis was performed to measure PC2 (n = 6/group) and PC1 (n = 6/group). These results were repeated in a separate experiment with the same response, n = 6/condition. *K* and *L,* intracellular (n = 6/group) and released (n = 4/group) CRH production. Data are mean ± S.E. *, p value < 0.05; **, p value < 0.01; ***, p value < 0.001.

observed no effect of FoxO1 on PC1 in the earlier mentioned experiments in N43-5 cells, and because our *in vivo* results strongly suggest that PVN Sirt1 regulates PC2 but not PC1.

In AtT20 cells, FoxO1 overexpression increased PC2 levels in a dose-dependent manner (Fig. 9*E*). However, FoxO1 also induced the expression of Sirt1 (Fig. 9*D*) consistent with previous studies (53). Therefore, to elucidate whether FoxO1 is indeed a positive regulator of PC2, or whether PC2 was induced by FoxO1 acting on Sirt1 and in turn on PC2, AtT20 cells were transfected to overexpress FoxO1 followed by inhibition of Sirt1 activity or vehicle control (Fig. 9*F*), which showed no changes in total FoxO1. However, inhibiting Sirt1 activity in the presence of FoxO1 overexpression resulted in increased acetylated FoxO1 (an indicator of decreased activity) (Fig. 9*G*) and was sufficient to mitigate the FoxO1-mediated increase in PC2 (Fig. 9, *H* and *I*). These results suggest that first FoxO1 is involved in the regulation of *preproPC2*, but also, depending on the metabolic state FoxO1 regulation of Sirt1, is necessary to regulate *preproPC2* (see Fig. 9, *G–I,* and Fig. 10). However, in these experiments, cells do not carry the *preproPC2* original

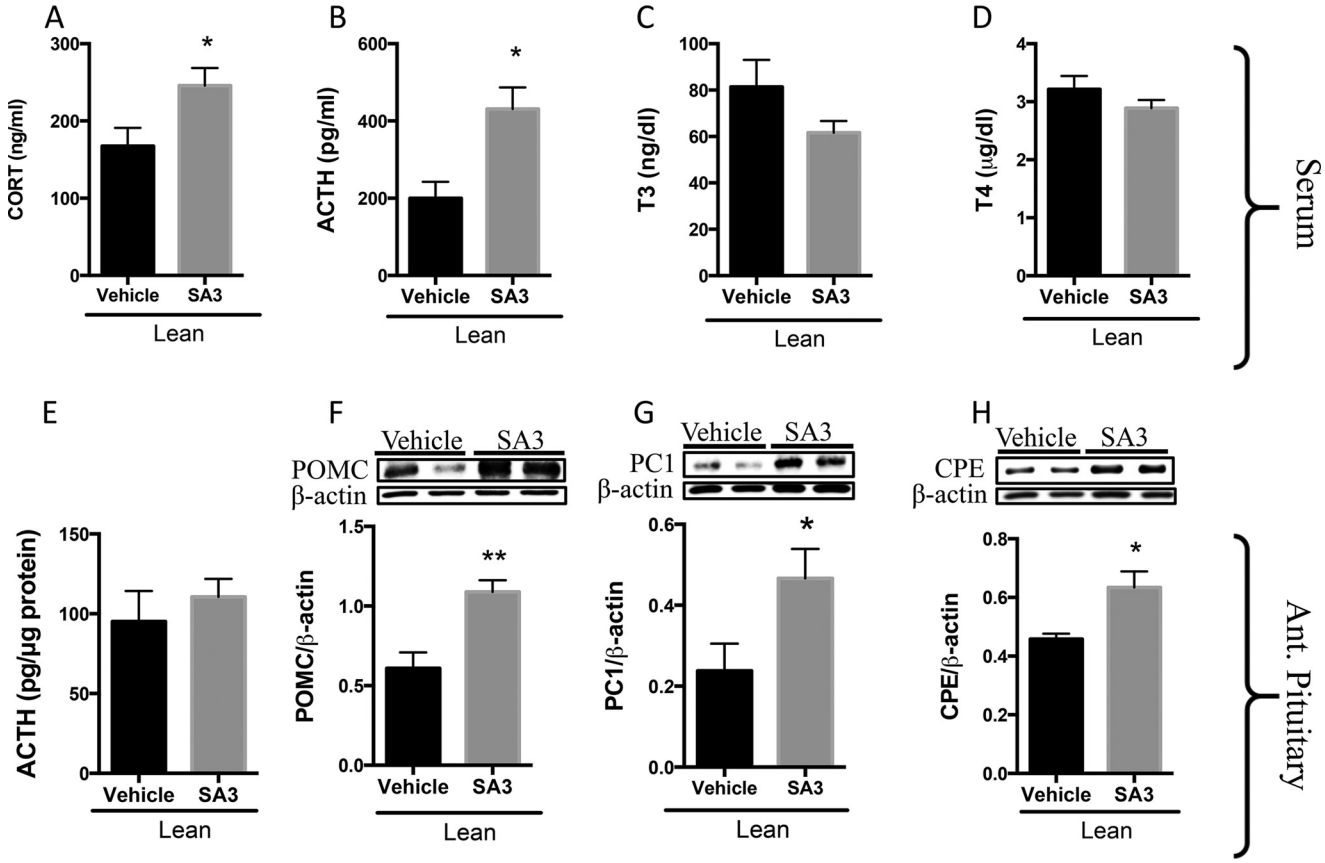

FIGURE 5. **PVN Sirt1 activation enhances adrenal activity in lean rats.** *A–H,* lean rats were intra-PVN-infused with SA3 (6 μg/rat) or vehicle beginning at 4 p.m. on day 1 and once more beginning at 10 a.m. the following day. Rats were sacrificed 3 h later. Trunk blood was collected, and serum was isolated and analyzed for parameters indicative of adrenal and thyroid activity and adenohypophysis analyzed for protein. *A,* GC ($n = 9$ vehicle and 11 SA3). *B,* ACTH ($n = 4$/group). *C,* T_3 ($n = 7$ vehicle and 9 SA3), and *D,* T_4 ($n = 7$ vehicle and 9 SA3). *E–H,* anterior pituitary was dissected and assayed by RIA for *E*. ACTH ($n = 4$ vehicle and 6 SA3) and by Western blot for *F*. POMC ($n = 7$ vehicle and 9 SA3); *G,* PC1 ($n = 5$ vehicle and 6 SA3);and *H,* CPE ($n = 5$ vehicle and 6 SA3). Data are mean ± S.E. *, p value < 0.05; **, p value < 0.01.

promoter, and we speculate that Sirt1 may signal via FoxO1 to augment both pro-PC2 and active PC2 levels and that FoxO1 may mediate Sirt1's post-translational effects on pro-PC2. In future studies, we will address some of these specific questions using specific genetic mouse models.

Discussion

This study shows the first evidence supporting the hypothesis that PVN Sirt1 activates the HPA axis and basal GC levels by enhancing the production of CRH through an increase in the biosynthesis of PC2, which is essential in the maturation of CRH from its prohormone, pro-CRH. Additionally, in the DIO state PVN Sirt1 increases basal (not stress-induced) circulating GC in a manner independent of *preproCRH* transcriptional changes. Instead, Sirt1's effects on adrenal activity are mediated via a post-translational processing mechanism in concert with an increase in PC2. Increased CRH release from the PVN increased pituitary ACTH synthesis and release, and in turn it increased circulating basal GC concentrations (Figs. 1 and 10). Using the combination of two *in vitro* systems (N43 and AtT20 cells), where Sirt1 was either cDNA overexpressed or inhibited by shRNA, we validated the proposed hypothesis that increased Sirt1 activity positively regulates PC2. Our *in vivo* studies support the assertion that Sirt1 significantly regulates PVN PC2. We also show that Sirt1 increased CRH production and release (Figs. 3, *E–H,* and 4, *A–H*). Although these results demonstrate that Sirt1 regulates PC1 and PC2 expression in a positive manner, we did not investigate the independent contributions of each convertase on the Sirt1-mediated processing of pro-CRH. However, it is worthy of noting that although AtT20 cells have been used to characterize the processing of pro-CRH by PC1, these cells are adrenocorticotropic in nature and can be influenced by CRH signaling (51). Thus, Sirt1's effect on PC1 may be a secondary consequence to changes in secreted CRH in the *in vitro* system employed.

Our *in vivo* data demonstrate that stimulating Sirt1 activity in the PVN of lean (Fig. 5) and DIO (Fig. 6) rodents results in elevated serum basal ACTH and GC levels. We were unable to assess PVN and ME for CRH content; however, we assessed the anterior pituitaries for changes in POMC, CPE, and PC1 as their expressions are induced in corticotroph cells upon CRH-mediated stimulation of the CRHR1. We observed an increase in POMC, PC1, and CPE expressed in the anterior pituitary of rodents with PVN Sirt1 stimulation. Together, these findings suggest that increasing PVN Sirt1 activity results in an increase in the amount of CRH targeted to the anterior pituitary, thereby enhancing ACTH signaling and basal GC concentration. Furthermore, our results demonstrate that inhibiting Sirt1 specifically in the PVN of obese rodents caused a reduction in PVN

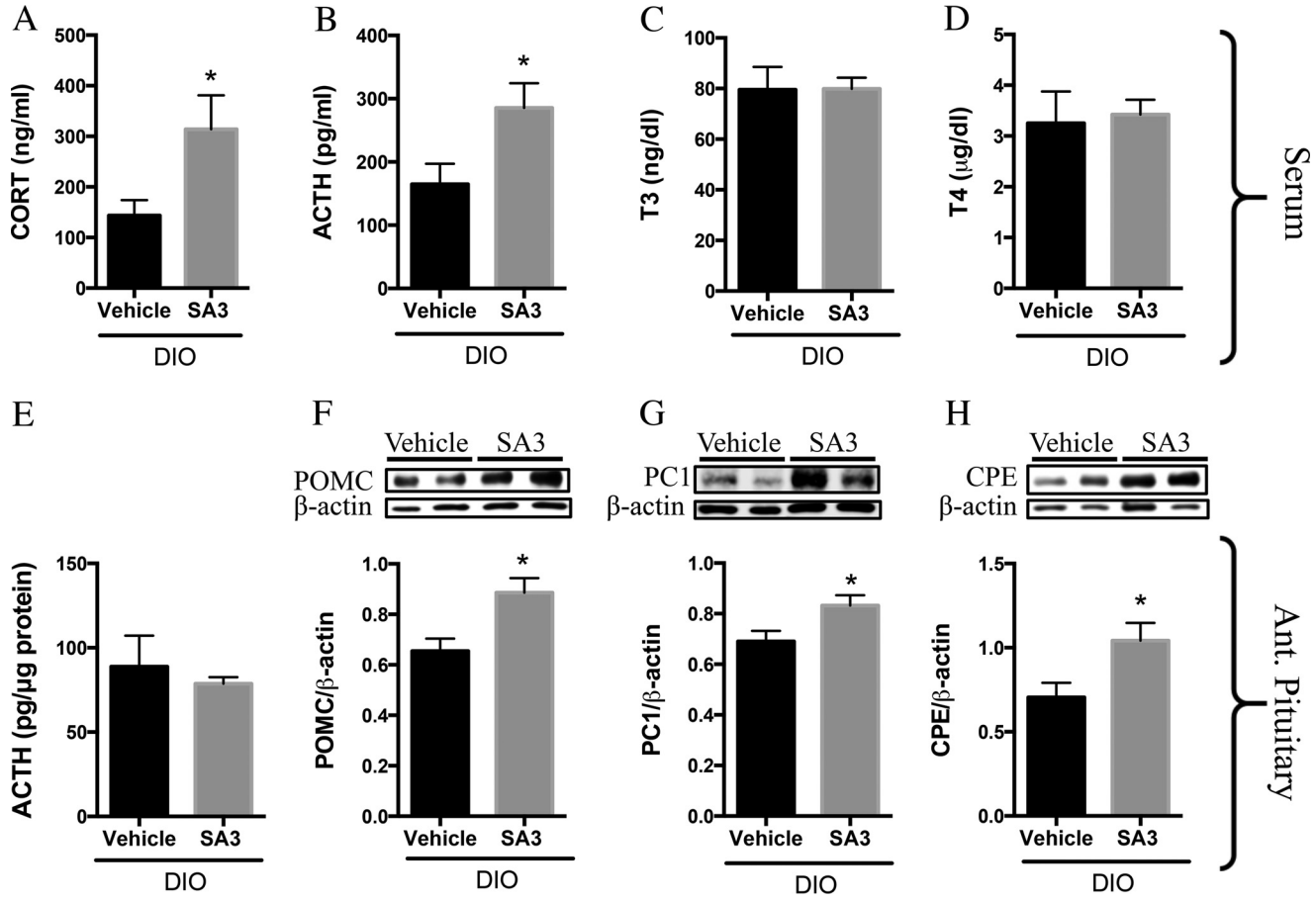

FIGURE 6. **PVN Sirt1 activation enhances adrenal activity in DIO rats.** DIO rats were intra-PVN-infused with SA3 (3–6 μg) or vehicle beginning at 3 p.m. on day 1 and once more beginning at 9 a.m. the following day. Rats were sacrificed a few hours later. *A–D,* trunk blood was collected, and serum was isolated and analyzed for parameters indicative of adrenal and thyroid activity. *A,* GC ($n = 7$ vehicle and 9 SA3). *B,* ACTH ($n = 4$ vehicle and 5 SA3). *C,* T_3 ($n = 8$ vehicle and 9 SA3), and *D,* T_4 ($n = 8$ vehicle and 9 SA3). *E*, anterior pituitary was dissected and assayed by RIA. *F*, anterior pituitary was assayed by Western blot for POMC. POMC ($n = 6$/group). *G,* PC1 ($n = 5$ vehicle and 6 SA3), and *H,* CPE ($n = 4$/group). Data are mean ± S.E. *, p value < 0.05.

pro-PC2 and active forms of PC2, but not PC1, protein (Fig. 8*A*). This decrease in PC2 was associated with a decrease in CRH in the ME (Fig. 8*E*), as well as reduced circulating GC (Fig. 8*F*), effects that were not observed in lean individuals (Fig. 7). *In vitro* data support these finding as increasing Sirt1 activity enhanced PC2 levels and CRH production, whereas diminished Sirt1 activity decreased PC2 levels and CRH production.

In terms of the possible mechanism regulating PC2, we found that the increase of the transcription factor FoxO1 in N43 cells up-regulated PC2 protein but not PC1. In further support, we showed that Sirt1 inhibition reduced the levels of deacetylated FoxO1 along with PC2 levels suggesting an important role for FoxO1 in regulating PC2. However, because FoxO1 also functions as a positive transcriptional regulator of Sirt1 (Fig. 9*H*), we were unable to reconcile whether these effects were a direct effect or a secondary effect of altered Sirt1 levels. Thus, we cannot exclude the possibility that FoxO1 acts upstream of Sirt1 to alter PC2. Future studies will investigate the extent to which each of these mechanisms regulates PC2 and CRH levels. Overall, our data suggest that Sirt1 in the DIO PVN specifically increases PC2, which increases CRH to ultimately elevate circulating levels of basal GC. Our preliminary results from PC2 promoter activity studies suggested that Sirt1 up-regulated PC2 (data not shown), which may suggest a direct action of Sirt1 on PC2 in addition to FoxO1 either acting on Sirt1 or directly on PC2. However, gene expression may not fully reflect altered protein or peptide content. For example, hypothalamic Sirt1 protein is increased during calorie deprivation, yet the *Sirt1* transcript is unaltered (36, 38). In addition, *preproPC2* mRNA, but not protein, is reduced under conditions of nutrient depletion (49). Results of this study reveal that Sirt1 stimulation induced the expression of PC1 and PC2 at the protein level, which complements the promoter activity data but not at the same ratio. This is supported by the well known fact that changes in promoter activity do not necessarily correlate directly to protein biosynthesis, a mechanism that is mostly controlled by a cell biology mechanism (folding, post-translational modifications, intracellular traffic, etc.). In addition to evidence that Sirt1 alters PC1 and PC2 promotor activity, we also observed that augmented Sirt1 increases endogenous levels of both pro-PC1 and pro-PC2 in N43-5 cells. The Sirt1-induced changes in PC2 using AtT20 cells further suggest that Sirt1 may affect PC2 at a post-translational level by an unknown mechanism. Additionally, central inhibition of Sirt1 caused a decrease in both pro-PC2 and the active form of PC2 in the DIO PVN, but the magnitude of decrease in active PC2 was greater (Fig. 8*N*). In addition, the maturation of PC2 to its active form can be regulated by many factors, including levels and activity

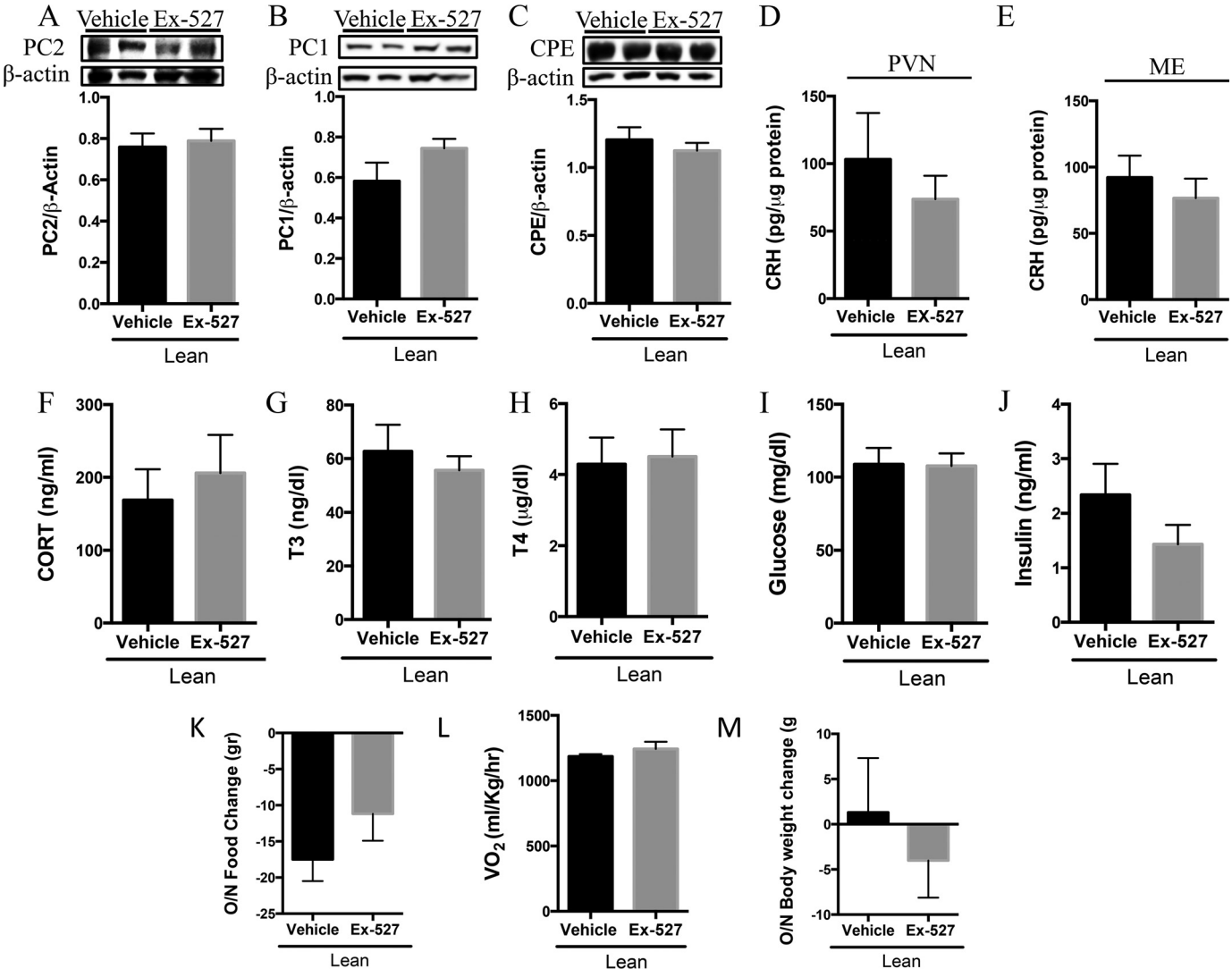

FIGURE 7. **PVN Sirt1 inhibition does not augment adrenal activity nor body weight in lean rats.** Lean rats were intra-PV-infused with 5 μg of Ex-527 or vehicle control beginning at 4 p.m. on day 1 and beginning at 11 a.m. the following morning. Rats were sacrificed a few hours later, and PVN was collected and subjected to Western blotting analysis for protein measurement, and serum was isolated and analyzed for hormones indicative of adrenal and thyroid activity. *A*, PC2 (n = 5/group); *B*, PC1 (n = 5/group); and *C*, CPE (n = 6 vehicle and 7 Ex-527) protein. *D* and *E*, CRH was measured by RIA in *D*. PVN (n = 5 vehicle and 7 Ex-527) and *E*, ARC/ME (n = 6 vehicle and 8 Ex-527). *F–J*, serum analysis for *F*. GC (n = 6 vehicle and 5 Ex-527). *G*, T_3 (n = 6 vehicle and 7 Ex-527). *H*, T_4 (n = 6 vehicle and 7 Ex-527). *I*, glucose (n = 9 vehicle and 6 Ex-527). *J*, insulin (n = 7/group). *K*, net change in the amount of food consumed (n = 6 vehicle and 8 Ex-527). *L*, overnight oxygen consumption (n = 3 vehicle and 5 Ex-527), *M*, net change in overnight body weight (n = 6 vehicle and 8 Ex-527). Data are mean ± S.E.

of the "chaperone"-like protein 7B2 and pH conditions in the secretory pathway. Future studies will explore how Sirt1 affects PC2 maturation.

Because we observed a significant decrease in plasma GC levels with Sirt1 inhibition in the PVN, we also assessed whether reduced adrenal activity would confer changes in energy balance. However, potentially due to the acute experimental paradigms used, we did not observe alterations in overnight food intake or energy expenditure (Fig. 8, *K* and *L*), yet these animals exhibited a net loss in body weight (Fig. 8*M*). We were unable to reconcile the cause of body weight loss in this study; however, future studies will investigate the mechanism mediating this effect. The aforementioned observation is in contrast to the reported effects of acute central Sirt1 manipulation, long term ARC Sirt1 knockdown, and chronic cell type-specific Sirt1 ablation models, wherein Sirt1 activity altered energy balance and body weight by affecting food intake, energy expenditure, sympathetic tone, and body fat composition (36, 37, 40, 41, 54–57). Moreover, several metabolic parameters associated with energy homeostasis were also affected in the aforementioned studies, including glucose homeostasis, insulin and leptin signaling, and adipose tissue dynamics. As glucocorticoids play a critical role in glucose and insulin homeostasis, we assessed whether PVN Sirt1's effect on adrenal activity also influenced these parameters.

The results indicate that inhibition of PVN Sirt1 activity did not significantly alter sated glucose levels; however, there was a trend for decreased glucose in DIO rodents with PVN Sirt1 inhibition in DIO (Fig. 8*I*) individuals. However, it resulted in a significant increase in sated serum insulin in obese rats (Fig. 8*J*) in the face of reduced basal GC (Fig. 8*F*), an observation that was not evident in lean rats (Fig. 7*J*). Although not assessed in this study, we speculate that a rise in sated insulin concentration may serve to diminish elevated circulating glucose levels

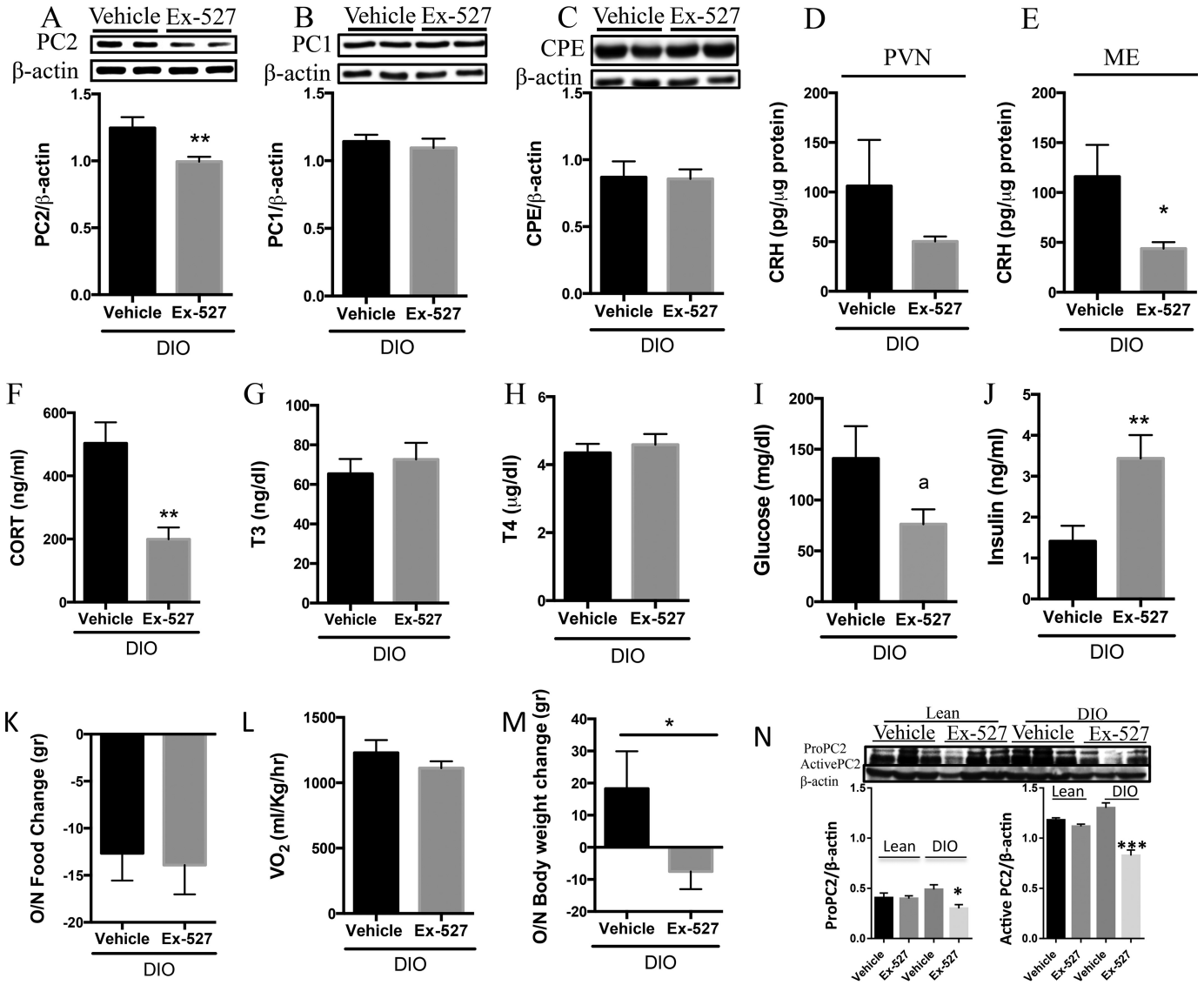

FIGURE 8. **PVN Sirt1 inhibition reduced adrenal activity in DIO.** DIO rats were intra-PVN-infused with 5 μg of Ex-527 or vehicle control beginning at 4 p.m. on day 1 and at 11 a.m. the following morning. Rats were sacrificed a few hours later, and serum and PVN were collected and analyzed. *A–C,* protein analysis in PVN samples. *A,* PC2 ($n = 7$ vehicle and 9 Ex-527). *B,* PC1 ($n = 4$/group) and CPE ($n = 7$ vehicle and 9 Ex-527) protein. *D* and *E,* CRH measured by RIA in *D*. PVN ($n = 4$ vehicle and 7 Ex-527), and *E,* ARC/ME ($n = 4$ vehicle and 5 Ex-527). *F–J,* serum analysis for *F*. GC ($n = 5$ vehicle and 8 Ex-527). *G,* T3 ($n = 3$ vehicle and 6 Ex-527). *H,* T4 ($n = 3$ vehicle and 6 Ex-527). *I,* glucose ($n = 11$ vehicle and 10 Ex-527). *J,* insulin ($n = 11$ vehicle and 12 Ex-527). *K,* net change in the amount of food consumed ($n = 6$ vehicle and 7 Ex-527). *L,* overnight oxygen consumption ($n = 3$ vehicle and 5 Ex-527). *M,* net change in overnight body weight ($n = 6$ vehicle and 11 Ex-527), and *N,* lean and DIO rats were icv-infused with vehicle or Ex-527 (as in Fig. 1), and PVN was collected and analyzed for pro-PC2 and PC2 levels ($n = 3$/group). Data are mean ± S.E. *, p value < 0.05; **, p value < 0.01; ***, p value < 0.001.

with time and may precede enhanced insulin sensitivity. Indeed, Lu *et al.* (41) demonstrated that a loss of functional Sirt1 in neurons of the central nervous system enhanced both brain and peripheral insulin sensitivity and reversed the hyperglycemia associated with obesity. However, Knight *et al.* (58) demonstrated that an acute increase in the activity of Sirt1 in the medial ARC of lean rats was sufficient to improve glucose homeostasis and increase insulin sensitivity. Collectively, these findings support a role of brain Sirt1 in regulating insulin and glucose homeostasis and point to region- and cell-specific influences in this regulation. Future studies are aimed at chronically reducing PVN Sirt1 activity to ascertain whether this will indeed alter glucose and insulin dynamics and/or have a substantial effect on energy balance.

In vivo data from other laboratories strongly support a role of PC2 in modulating CRH production. Under basal conditions, CRH neurons primarily express PC2, which is the likely PC responsible for the enzymatic processing of pro-CRH into CRH (59). However, CRH expressing neurons do express minute levels of PC1, and its expression is up-regulated under conditions of acute stress and glucocorticoid insufficiency (65). In addition, arginine vasopressin (AVP) cells of the PVN also express PC1, and both PC2 and PC1 equally processes pro-AVP (65). We did not investigate the involvement of AVP in the context of Sirt1 regulation of the HPA axis in this study. However, it is possible that Sirt1's positive regulation of the PCs enhances basal adrenal activity by affecting both CRH and AVP production, although the latter remains unknown.

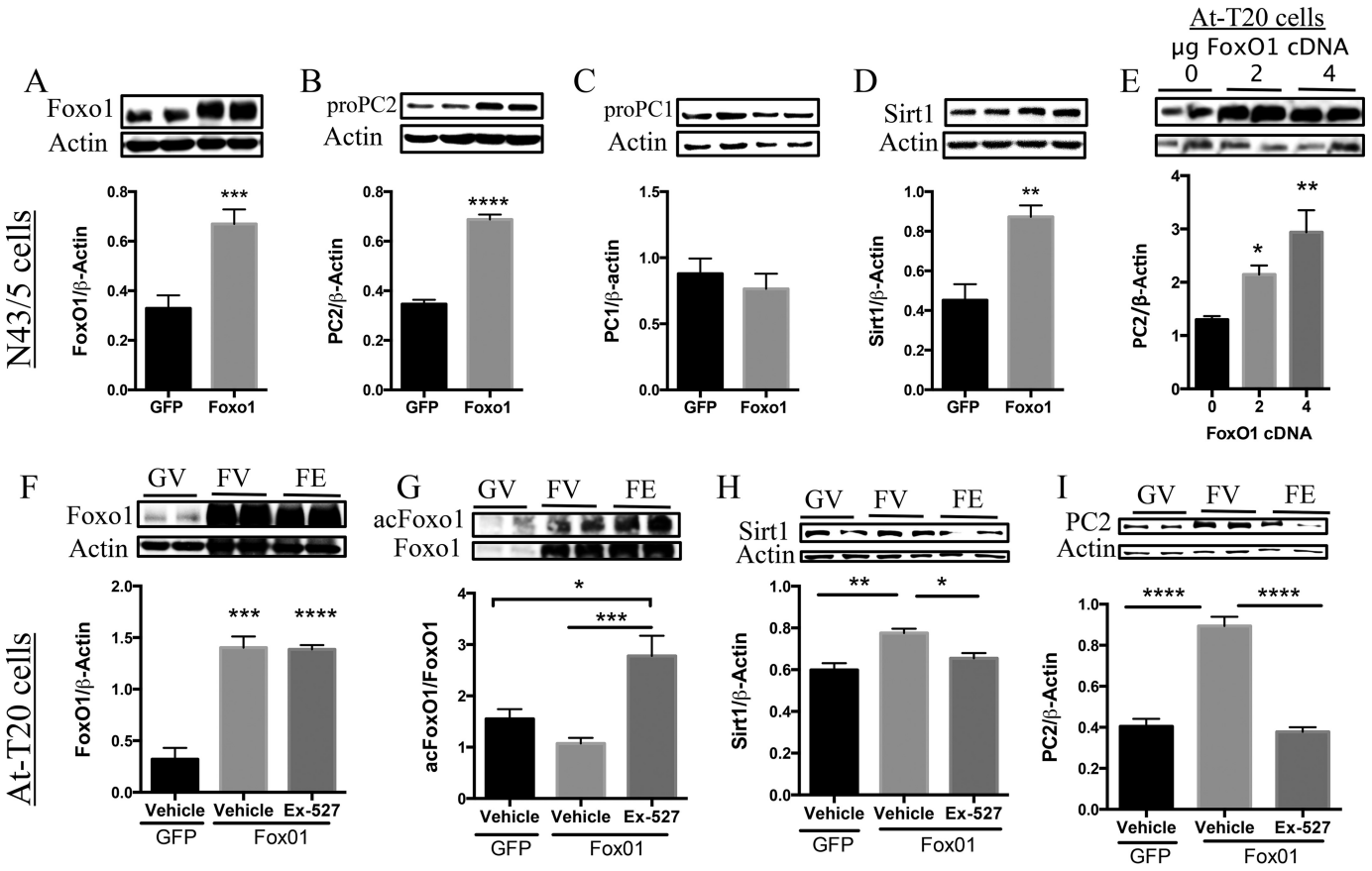

FIGURE 9. **FoxO1 mediates PC2 production.** *A–D*, N43-5 cells were transfected with either 4 μg of GFP cDNA or FoxO1 cDNA ($n = 6$/group) and were collected 48 h post-transfection. *A,* FoxO1 protein. *B,* PC1 protein. *C,* PC2 protein. *D,* Sirt1 protein levels measured by Western blotting analysis. These results were repeated in an independent experiment with a similar response ($n = 6$/group). *E–H,* in another experiment, AtT20 cells were transfected as just described and were treated with Ex-527 (50 μM) or with vehicle control for 6 h and collected 48 h post-transfection. *E,* PC2 protein ($n = 12$/group); *F,* FoxO1 protein ($n = 6$/group); *G,* acFoxO1 protein ($n = 6$/group); *H,* Sirt1 ($n = 9$ GFP-vehicle (*GV*), 13 FoxO1-vehicle (*FV*), and 7 FoxO1-Ex527 (*FE*)); *I,* PC2 protein ($n = 9$ GFP-vehicle (*GV*), 12 FoxO1-vehicle (*FV*), and 12 FoxO1-Ex527 (*FE*), and protein levels were measured by Western blotting analysis. Data are mean ± S.E. *, p value< 0.05; **, p value < 0.01; ***, p value < 0.001; ****, p value < 0.0001.

The observation that no changes in PVN PC1 protein in rodents with central Sirt1 inhibition (Fig. 1, *H* and *K*) and in contrast to our *in vitro* results may be explained by the following. As aforementioned, DIO rats with central Sirt1 inhibition display increased α-MSH that results in enhanced activation of TRH neurons (40). Furthermore, PC1 is enhanced upon stimulation of the TRH neuron (49). As we failed to examine cell-specific fluctuations in PC1 and PC2 upon Sirt1 manipulation, and instead analyzed PVN micropunches for PC content, it is possible that a down-regulation in PC1 (presumably in CRH neurons) due to central Sirt1 inhibition may be offset by α-MSH's induction of PVN PC1 (presumably in TRH neurons). Alternatively, glucocorticoid receptor resistance has also been reported in obese individuals (60, 61), and a study revealed that adrenalectomy increased the expression of PC1 in hypophysiotropic CRH neurons, an effect that was blunted via administration of exogenous GCs (59). We have shown previously that Sirt1 in the ARC regulates, at the central level, the thyroid axis via its actions on several components of the central melanocortin system (36, 40). Our prior studies revealed that central Sirt1 inhibition increased ARC α-MSH production, an effect that was mediated via increased ARC CPE protein. This resulted in an increase in hypophysiotropic thyroid activity in obese individuals; however, we failed to investigate its effect on the HPA axis in those prior studies.

α-MSH is also targeted to CRH neurons of the PVN and augments energy balance in part by activation of CRH neurons, which is mediated by transcription of the *CRH* gene (62, 63). Thus, in this study, we indirectly assessed whether α-MSH was mediating the effects of central Sirt1 on the hypophysiotropic adrenal axis by assessing CRH mRNA in PVN. There was no difference in CRH mRNA levels from the PVN of individuals centrally infused to inhibit Sirt1 activity when compared with their vehicle-infused controls, suggesting that α-MSH's induction of *CRH* transcription did not occur. α-MSH's effect on energy balance, particularly feeding, is in part facilitated through CRH signaling (54). As we observed no effect of central Sirt1 inhibition on feeding in DIO rodents (40), it is likely that α-MSH was preferentially targeted to TRH neurons as evidenced by enhanced thyroid activity and energy expenditure (40), a proposition that is under current investigation. In addition to its regulation of the hypophysiotropic thyroid axis, a recent study has revealed a role of central Sirt1 in regulating the hypophysiotropic gonadal axis. Sirt1 was shown to mediate Leydig and Sertoli cell maturity by regulating steroidogenic gene expression and, in particular, at the central level by

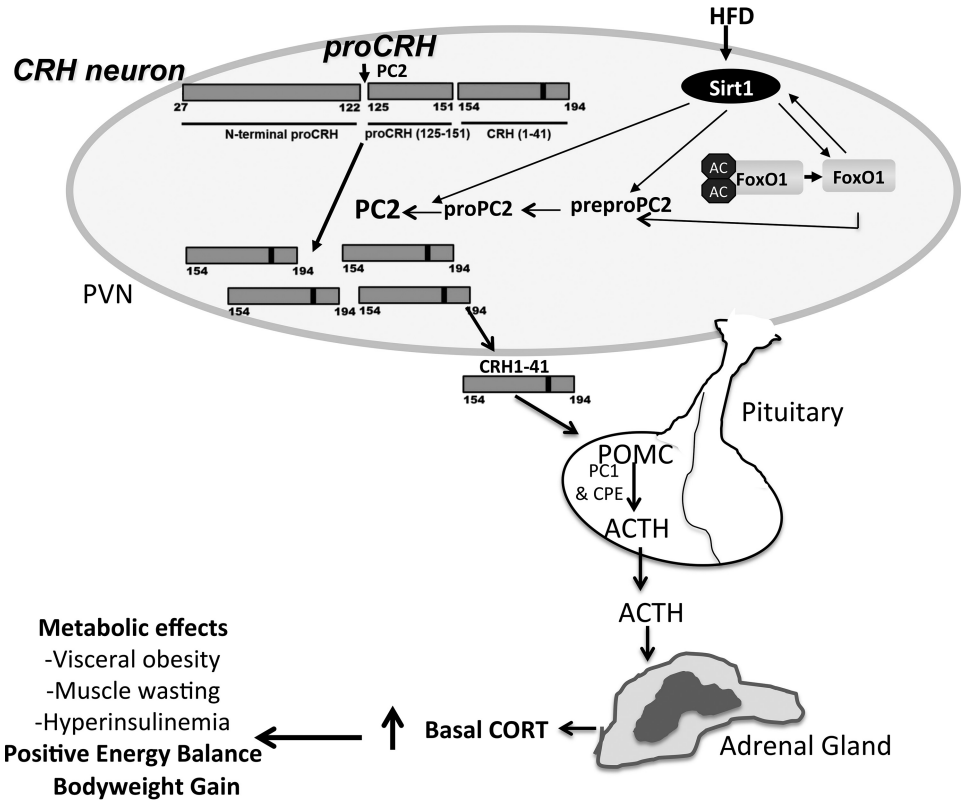

FIGURE 10. **Model depicting the proposed PVN Sirt1's regulation in the hypophysiotropic adrenal axis.** Feeding a high fat diet results in increased Sirt1 protein in the PVN. Sirt1 increases levels of both pro-PC2 and active PC2. The effect of Sirt1 on PC2 appears to also be mediated by FoxO1, but the extent of FoxO1's role remains unknown. PC2 in turn acts on pro-CRH, thus increasing CRH output to the hypophyseal portal system. This results in stimulation of POMC biosynthesis and processing leading to increased production and release of ACTH by corticotroph cells of the anterior pituitary. ACTH then acts on the adrenal cortex, stimulating the production and release of GC, thereby promoting a positive energy balance that may ultimately lead to excessive weight gain if unresolved. *AC,* acetyl; *black bars* in the pro-CRH molecule indicate the site of pair of basic residues; *HFD,* high fat diet; *PVN,* paraventricular nucleus of the hypothalamus. *Arrows* directed to PC2 from Sirt1 and FoxO1 indicate the suggested possible actions on prepro-PC2 gene and pro-PC2 protein post-translational processing.

increasing the expression of gonadotropin-releasing hormone, thereby resulting in increased circulating luteinizing hormone and intratesticular testosterone levels (64).

Another study (65) revealed that a peripheral administration of resveratrol resulted in reduced GC in a chronic unpredictable mild stress model that is characterized by hyperactivity of the HPA axis. Although it is possible that resveratrol could act through Sirt1 to mediate the aforementioned effects, the investigators did not examine Sirt1's involvement in this process. Sirt1's involvement in down-regulating HPA activity at first would seem to contradict the observations presented in this study; however, the down-regulatory effects of resveratrol on hypophysiotropic adrenal activity was attributed by the authors of that study to resveratrol action in the periphery rather than in the brain (65). Sirt1, like many other metabolic sensors (*i.e.* AMP-activated kinase and mechanistic target of rapamycin), has opposing roles in the brain *versus* its functions in the periphery. Generally, Sirt1 action in the periphery functions to promote a negative energy balance and to protect against the development of metabolic dysfunctions and obesity. In the hypothalamus, Sirt1's role remains opaque, yet a number of studies have demonstrated central Sirt1 to promote a positive energy balance. Future studies will employ the use of genetic models to ascertain the specific role of Sirt1 expressed in CRH neurons of the PVN in regard to energy balance and its regulation of the HPA axis. Collectively, the findings demonstrate that Sirt1 regulates the CRH peptide by modulating the processing enzyme PC2 and FoxO1 adding a novel regulatory link between PVN Sirt1 and HPA axis activity.

Author Contributions—E. A. N., A. M. T., and N. E. C. designed the study and wrote the paper. A. M. T. and N. E. C. designed, performed, and analyzed the experiments shown in Figs. 1 and 9. A. M. T. and N. E. C. designed and R. B. performed and analyzed the experiments in Fig. 2. A. M. T. and E. A. N. designed, performed, and analyzed the experiments in Figs. 3–8. J. S. S. and G. F. provided technical assistance and contributed to the preparation of figures. All authors reviewed the results and approved the final version of the manuscript. The final revision was done and approved by E. A. N.

Acknowledgments—We thank Ronald Stuart, Claudia Arevalo, Lindsay Steele, Katherine Barcay, and Ashleigh Burton for technical assistance.

References

1. Vale, W., Spiess, J., Rivier, C., and Rivier, J. (1981) Characterization of a 41-residue ovine hypothalamic peptide that stimulates secretion of corticotropin and β-endorphin. *Science* **213,** 1394–1397
2. Kovács, K. J. (2013) CRH: the link between hormonal-, metabolic- and behavioral responses to stress. *J. Chem. Neuroanat.* **54,** 25–33
3. Sominsky, L., and Spencer, S. J. (2014) Eating behavior and stress: a path-

way to obesity. *Front. Psychol.* **5,** 434
4. Chrousos, G. P. (1995) The hypothalamic-pituitary-adrenal axis and immune-mediated inflammation. *N. Engl. J. Med.* **332,** 1351–1362
5. Seimon, R. V., Hostland, N., Silveira, S. L., Gibson, A. A., and Sainsbury, A. (2013) Effects of energy restriction on activity of the hypothalamo-pituitary-adrenal axis in obese humans and rodents: implications for diet-induced changes in body composition. *Horm. Mol. Biol. Clin. Investig.* **15,** 71–80
6. Ziegler, C. G., Krug, A. W., Zouboulis, C. C., and Bornstein, S. R. (2007) Corticotropin-releasing hormone and its function in the skin. *Horm. Metab. Res.* **39,** 106–109
7. Raadsheer, F. C., Sluiter, A. A., Ravid, R., Tilders, F. J., and Swaab, D. F. (1993) Localization of corticotropin-releasing hormone (CRH) neurons in the paraventricular nucleus of the human hypothalamus; age-dependent colocalization with vasopressin. *Brain Res.* **615,** 50–62
8. Korosi, A., and Baram, T. Z. (2008) The central corticotropin releasing factor system during development and adulthood. *Eur. J. Pharmacol.* **583,** 204–214
9. Aguilera, G., Subburaju, S., Young, S., and Chen, J. (2008) The parvocellular vasopressinergic system and responsiveness of the hypothalamic pituitary adrenal axis during chronic stress. *Prog. Brain Res.* **170,** 29–39
10. Nillni, E. A. (2007) Regulation of prohormone convertases in hypothalamic neurons: implications for prothyrotropin-releasing hormone and proopiomelanocortin. *Endocrinology* **148,** 4191–4200
11. Steiner, D. F. (1998) The proprotein convertases. *Curr. Opin. Chem. Biol.* **2,** 31–39
12. Nillni, E. A., Xie, W., Mulcahy, L., Sanchez, V. C., and Wetsel, W. C. (2002) Deficiencies in pro-thyrotropin-releasing hormone processing and abnormalities in thermoregulation in Cpefat/fat mice. *J. Biol. Chem.* **277,** 48587–48595
13. Lloyd, D. J., Bohan, S., and Gekakis, N. (2006) Obesity, hyperphagia and increased metabolic efficiency in Pc1 mutant mice. *Hum. Mol. Genet.* **15,** 1884–1893
14. Naggert, J. K., Fricker, L. D., Varlamov, O., Nishina, P. M., Rouille, Y., Steiner, D. F., Carroll, R. J., Paigen, B. J., and Leiter, E. H. (1995) Hyperinsulinemia in obese fat/fat mice associated with a carboxypeptidase E mutation which reduces enzyme activity. *Nat. Genet.* **10,** 135–142
15. Jing, E., Nillni, E. A., Sanchez, V. C., Stuart, R. C., and Good, D. J. (2004) Deletion of the Nhlh2 transcription factor decreases the levels of the anorexigenic peptides α-melanocyte-stimulating hormone and thyrotropin-releasing hormone and implicates prohormone convertases I and II in obesity. *Endocrinology* **145,** 1503–1513
16. Jackson, R. S., Creemers, J. W., Ohagi, S., Raffin-Sanson, M. L., Sanders, L., Montague, C. T., Hutton, J. C., and O'Rahilly, S. (1997) Obesity and impaired prohormone processing associated with mutations in the human convertase 1 gene. *Nat. Genet.* **16,** 303–306
17. Challis, B. G., Pritchard, L. E., Creemers, J. W., Delplanque, J., Keogh, J. M., Luan, J., Wareham, N. J., Yeo, G. S., Bhattacharyya, S., Froguel, P., White, A., Farooqi, I. S., and O'Rahilly, S. (2002) A missense mutation disrupting a dibasic prohormone processing site in pro-opiomelanocortin (POMC) increases susceptibility to early-onset obesity through a novel molecular mechanism. *Hum. Mol. Genet.* **11,** 1997–2004
18. Spiess, J., Rivier, J., Rivier, C., and Vale, W. (1981) Primary structure of corticotropin-releasing factor from ovine hypothalamus. *Proc. Natl. Acad. Sci. U.S.A.* **78,** 6517–6521
19. Rivier, J., Spiess, J., and Vale, W. (1983) Characterization of rat hypothalamic corticotropin-releasing factor. *Proc. Natl. Acad. Sci. U.S.A.* **80,** 4851–4855
20. Perone, M. J., Murray, C. A., Brown, O. A., Gibson, S., White, A., Linton, E. A., Perkins, A. V., Lowenstein, P. R., and Castro, M. G. (1998) Procorticotrophin-releasing hormone: endoproteolytic processing and differential release of its derived peptides within AtT20 cells. *Mol. Cell. Endocrinol.* **142,** 191–202
21. Brar, B., Sanderson, T., Wang, N., and Lowry, P. J. (1997) Post-translational processing of human procorticotrophin-releasing factor in transfected mouse neuroblastoma and Chinese hamster ovary cell lines. *J. Endocrinol.* **154,** 431–440
22. Castro, M., Lowenstein, P., Glynn, B., Hannah, M., Linton, E., and Lowry, P. (1991) Post-translational processing and regulated release of corticotropin-releasing hormone (CRH) in AtT20 cells expressing the human pro-CRH gene. *Biochem. Soc. Trans.* **19,** 246S
23. Eipper, B. A., Milgram, S. L., Husten, E. J., Yun, H. Y., and Mains, R. E. (1993) Peptidylglycine α-amidating monooxygenase: a multifunctional protein with catalytic, processing, and routing domains. *Protein Sci.* **2,** 489–497
24. Rho, J. H., and Swanson, L. W. (1987) Neuroendocrine CRF motoneurons: intrahypothalamic axon terminals shown with a new retrograde-Lucifer-immuno method. *Brain Res.* **436,** 143–147
25. Lovejoy, D. A., Chang, B. S., Lovejoy, N. R., and del Castillo, J. (2014) Molecular evolution of GPCRs: CRH/CRH receptors. *J. Mol. Endocrinol.* **52,** T43–T60
26. Solomon, S. (1999) POMC-derived peptides and their biological action. *Ann. N. Y. Acad. Sci.* **885,** 22–40
27. Veo, K., Reinick, C., Liang, L., Moser, E., Angleson, J. K., and Dores, R. M. (2011) Observations on the ligand selectivity of the melanocortin 2 receptor. *Gen. Comp. Endocrinol.* **172,** 3–9
28. Richard, D., Huang, Q., and Timofeeva, E. (2000) The corticotropin-releasing hormone system in the regulation of energy balance in obesity. *Int. J. Obes. Relat. Metab. Disord.* **24,** S36–S39
29. Mastorakos, G., and Zapanti, E. (2004) The hypothalamic-pituitary-adrenal axis in the neuroendocrine regulation of food intake and obesity: the role of corticotropin-releasing hormone. *Nutr. Neurosci.* **7,** 271–280
30. Toriya, M., Maekawa, F., Maejima, Y., Onaka, T., Fujiwara, K., Nakagawa, T., Nakata, M., and Yada, T. (2010) Long-term infusion of brain-derived neurotrophic factor reduces food intake and body weight via a corticotrophin-releasing hormone pathway in the paraventricular nucleus of the hypothalamus. *J. Neuroendocrinol.* **22,** 987–995
31. Tataranni, P. A., Larson, D. E., Snitker, S., Young, J. B., Flatt, J. P., and Ravussin, E. (1996) Effects of glucocorticoids on energy metabolism and food intake in humans. *Am. J. Physiol.* **271,** E317–E325
32. Laryea, G., Schütz, G., and Muglia, L. J. (2013) Disrupting hypothalamic glucocorticoid receptors causes HPA axis hyperactivity and excess adiposity. *Mol. Endocrinol.* **27,** 1655–1665
33. Kong, X., Yu, J., Bi, J., Qi, H., Di, W., Wu, L., Wang, L., Zha, J., Lv, S., Zhang, F., Li, Y., Hu, F., Liu, F., Zhou, H., Liu, J., and Ding, G. (2015) Glucocorticoids transcriptionally regulate miR-27b expression promoting body fat accumulation via suppressing the browning of white adipose tissue. *Diabetes* **64,** 393–404
34. Spencer, S. J., and Tilbrook, A. (2011) The glucocorticoid contribution to obesity. *Stress* **14,** 233–246
35. Cantó, C., Gerhart-Hines, Z., Feige, J. N., Lagouge, M., Noriega, L., Milne, J. C., Elliott, P. J., Puigserver, P., and Auwerx, J. (2009) AMPK regulates energy expenditure by modulating NAD^+ metabolism and SIRT1 activity. *Nature* **458,** 1056–1060
36. Cakir, I., Perello, M., Lansari, O., Messier, N. J., Vaslet, C. A., and Nillni, E. A. (2009) Hypothalamic Sirt1 regulates food intake in a rodent model system. *PLoS ONE* **4,** e8322
37. Dietrich, M. O., Antunes, C., Geliang, G., Liu, Z. W., Borok, E., Nie, Y., Xu, A. W., Souza, D. O., Gao, Q., Diano, S., Gao, X. B., and Horvath, T. L. (2010) Agrp neurons mediate Sirt1's action on the melanocortin system and energy balance: roles for Sirt1 in neuronal firing and synaptic plasticity. *J. Neurosci.* **30,** 11815–11825
38. Ramadori, G., Lee, C. E., Bookout, A. L., Lee, S., Williams, K. W., Anderson, J., Elmquist, J. K., and Coppari, R. (2008) Brain SIRT1: anatomical distribution and regulation by energy availability. *J. Neurosci.* **28,** 9989–9996
39. Kanfi, Y., Peshti, V., Gozlan, Y. M., Rathaus, M., Gil, R., and Cohen, H. Y. (2008) Regulation of SIRT1 protein levels by nutrient availability. *FEBS Lett.* **582,** 2417–2423
40. Cyr, N. E., Steger, J. S., Toorie, A. M., Yang, J. Z., Stuart, R., and Nillni, E. A. (2015) Central Sirt1 regulates body weight and energy expenditure along with the POMC-derived peptide α-MSH and the processing enzyme CPE production in diet-induced obese male rats. *Endocrinology* **156,** 961–974
41. Lu, M., Sarruf, D. A., Li, P., Osborn, O., Sanchez-Alavez, M., Talukdar, S., Chen, A., Bandyopadhyay, G., Xu, J., Morinaga, H., Dines, K., Watkins, S., Kaiyala, K., Schwartz, M. W., and Olefsky, J. M. (2013) Neuronal Sirt1

deficiency increases insulin sensitivity in both brain and peripheral tissues. *J. Biol. Chem.* **288,** 10722–10735
42. Levin, B. E., Dunn-Meynell, A. A., Balkan, B., and Keesey, R. E. (1997) Selective breeding for diet-induced obesity and resistance in Sprague-Dawley rats. *Am. J. Physiol.* **273,** R725–R730
43. Perello, M., Cakir, I., Cyr, N. E., Romero, A., Stuart, R. C., Chiappini, F., Hollenberg, A. N., and Nillni, E. A. (2010) Maintenance of the thyroid axis during diet-induced obesity in rodents is controlled at the central level. *Am. J. Physiol. Endocrinol. Metab.* **299,** E976–E989
44. Evanson, N. K., Van Hooren, D. C., and Herman, J. P. (2009) GluR5-mediated glutamate signaling regulates hypothalamo-pituitary-adrenocortical stress responses at the paraventricular nucleus and median eminence. *Psychoneuroendocrinology* **34,** 1370–1379
45. Himms-Hagen, J. (1997) On raising energy expenditure in ob/ob mice. *Science* **276,** 1132–1133
46. Cyr, N. E., Steger, J. S., Toorie, A. M., Yang, J. Z., Stuart, R., and Nillni, E. A. (2014) Central Sirt1 regulates body weight and energy expenditure along with the POMC-derived peptide α-MSH and the processing enzyme CPE production in diet-induced obese male rats. *Endocrinology* **155,** 2423–2435
47. Cyr, N. E., Toorie, A. M., Steger, J. S., Sochat, M. M., Hyner, S., Perello, M., Stuart, R., and Nillni, E. A. (2013) Mechanisms by which the orexigen NPY regulates anorexigenic α-MSH and TRH. *Am. J. Physiol. Endocrinol. Metab.* **304,** E640–E650
48. Rodgers, J. T., Lerin, C., Haas, W., Gygi, S. P., Spiegelman, B. M., and Puigserver, P. (2005) Nutrient control of glucose homeostasis through a complex of PGC-1α and SIRT1. *Nature* **434,** 113–118
49. Sanchez, V. C., Goldstein, J., Stuart, R. C., Hovanesian, V., Huo, L., Munzberg, H., Friedman, T. C., Bjorbaek, C., and Nillni, E. A. (2004) Regulation of hypothalamic prohormone convertases 1 and 2 and effects on processing of prothyrotropin-releasing hormone. *J. Clin. Invest.* **114,** 357–369
50. Wren, M. A., Dauchy, R. T., Hanifin, J. P., Jablonski, M. R., Warfield, B., Brainard, G. C., Blask, D. E., Hill, S. M., Ooms, T. G., and Bohm, R. P., Jr. (2014) Effect of different spectral transmittances through tinted animal cages on circadian metabolism and physiology in Sprague-Dawley rats. *J. Am. Assoc. Lab. Anim. Sci.* **53,** 44–51
51. Castro, M. G., Brooke, J., Bullman, A., Hannah, M., Glynn, B. P., and Lowry, P. J. (1991) Biosynthesis of corticotrophin-releasing hormone (CRH) in mouse corticotrophic tumour cells expressing the human pro-CRH gene: intracellular storage and regulated secretion. *J. Mol. Endocrinol.* **7,** 97–104
52. Plum, L., Lin, H. V., Dutia, R., Tanaka, J., Aizawa, K. S., Matsumoto, M., Kim, A. J., Cawley, N. X., Paik, J. H., Loh, Y. P., DePinho, R. A., Wardlaw, S. L., and Accili, D. (2009) The obesity susceptibility gene Cpe links FoxO1 signaling in hypothalamic pro-opiomelanocortin neurons with regulation of food intake. *Nat. Med.* **15,** 1195–1201
53. Xiong, S., Salazar, G., Patrushev, N., and Alexander, R. W. (2011) FoxO1 mediates an autofeedback loop regulating SIRT1 expression. *J. Biol. Chem.* **286,** 5289–5299
54. Ramadori, G., Fujikawa, T., Anderson, J., Berglund, E. D., Frazao, R., Michán, S., Vianna, C. R., Sinclair, D. A., Elias, C. F., and Coppari, R. (2011) SIRT1 deacetylase in SF1 neurons protects against metabolic imbalance. *Cell Metab.* **14,** 301–312
55. Ramadori, G., Fujikawa, T., Fukuda, M., Anderson, J., Morgan, D. A., Mostoslavsky, R., Stuart, R. C., Perello, M., Vianna, C. R., Nillni, E. A., Rahmouni, K., and Coppari, R. (2010) SIRT1 deacetylase in POMC neurons is required for homeostatic defenses against diet-induced obesity. *Cell Metab.* **12,** 78–87
56. Sasaki, T., Kikuchi, O., Shimpuku, M., Susanti, V. Y., Yokota-Hashimoto, H., Taguchi, R., Shibusawa, N., Sato, T., Tang, L., Amano, K., Kitazumi, T., Kuroko, M., Fujita, Y., Maruyama, J., Lee, Y. S., *et al.* (2014) Hypothalamic SIRT1 prevents age-associated weight gain by improving leptin sensitivity in mice. *Diabetologia* **57,** 819–831
57. Sasaki, T., Kim, H. J., Kobayashi, M., Kitamura, Y. I., Yokota-Hashimoto, H., Shiuchi, T., Minokoshi, Y., and Kitamura, T. (2010) Induction of hypothalamic Sirt1 leads to cessation of feeding via agouti-related peptide. *Endocrinology* **151,** 2556–2566
58. Knight, C. M., Gutierrez-Juarez, R., Lam, T. K., Arrieta-Cruz, I., Huang, L., Schwartz, G., Barzilai, N., and Rossetti, L. (2011) Mediobasal hypothalamic SIRT1 is essential for resveratrol's effects on insulin action in rats. *Diabetes* **60,** 2691–2700
59. Dong, W., Seidel, B., Marcinkiewicz, M., Chrétien, M., Seidah, N. G., and Day, R. (1997) Cellular localization of the prohormone convertases in the hypothalamic paraventricular and supraoptic nuclei: selective regulation of PC1 in corticotrophin-releasing hormone parvocellular neurons mediated by glucocorticoids. *J. Neurosci.* **17,** 563–575
60. de Guia, R. M., Rose, A. J., and Herzig, S. (2014) Glucocorticoid hormones and energy homeostasis. *Horm. Mol. Biol. Clin. Invest.* **19,** 117–128
61. Jessop, D. S., Dallman, M. F., Fleming, D., and Lightman, S. L. (2001) Resistance to glucocorticoid feedback in obesity. *J. Clin. Endocrinol. Metab.* **86,** 4109–4114
62. Dhillo, W. S., Small, C. J., Seal, L. J., Kim, M. S., Stanley, S. A., Murphy, K. G., Ghatei, M. A., and Bloom, S. R. (2002) The hypothalamic melanocortin system stimulates the hypothalamo-pituitary-adrenal axis *in vitro* and *in vivo* in male rats. *Neuroendocrinology* **75,** 209–216
63. Fekete, C., Légrádi, G., Mihály, E., Tatro, J. B., Rand, W. M., and Lechan, R. M. (2000) α-Melanocyte stimulating hormone prevents fasting-induced suppression of corticotropin-releasing hormone gene expression in the rat hypothalamic paraventricular nucleus. *Neurosci. Lett.* **289,** 152–156
64. Kolthur-Seetharam, U., Teerds, K., de Rooij, D. G., Wendling, O., McBurney, M., Sassone-Corsi, P., and Davidson, I. (2009) The histone deacetylase SIRT1 controls male fertility in mice through regulation of hypothalamic-pituitary gonadotropin signaling. *Biol. Reprod.* **80,** 384–391
65. Ge, J. F., Peng, L., Cheng, J. Q., Pan, C. X., Tang, J., Chen, F. H., and Li, J. (2013) Antidepressant-like effect of resveratrol: involvement of antioxidant effect and peripheral regulation on HPA axis. *Pharmacol. Biochem. Behav.* **114,** 64–69